NIST

NISTIR 3966

A CRYOGENIC 4.4 MN MECHANICAL TEST SYSTEM FOR LARGE SCALE TESTS OF COMPOSITE SUPPORT STRUTS

R.P. Walsh
R.P. Reed
J.D. McColskey
W. Fehringer
J.R. Berger

NISTIR 3966

A CRYOGENIC 4.4 MN MECHANICAL TEST SYSTEM FOR LARGE SCALE TESTS OF COMPOSITE SUPPORT STRUTS

R.P. Walsh
R.P. Reed
J.D. McColskey
W. Fehringer
J.R. Berger

Materials Reliability Division
Materials Science and Engineering Laboratory
National Institute of Standards and Technology
Boulder, Colorado 80303

March 1992

TABLE OF CONTENTS

1.0 EXECUTIVE SUMMARY

The mechanical tests reported here were conducted by the Materials Reliability Division of the National Institute of Standards and Technology. These tests were intended to validate the full scale structural behavior of fiber reinforced polymer (FRP) support struts in a thermal and mechanical environment similar to the actual service conditions.

Two types of tests were performed: ultimate compressive strength and fatigue. Thermal conditions for the tests ranged from isothermal room temperature tests to an imposed thermal gradient of cryogenic-to-room temperatures. The development of the unique facility necessary for the large scale cryogenic tests is detailed in this report.

A summary of all tests is presented in Table 1. Many tests demonstrated that a problem exists with the aluminum alloy (7075-T6) end fittings. Failure seemed to propagate from the failed end fittings into the tube, thereby preventing the tube from reaching its theoretical ultimate strength.

2.0   INTRODUCTION

The superconducting magnetic energy storage (SMES) coil magnet requires an array of large radial compression members to resist dimensional change of the coil. The design for the compression members uses FRP composite tubes. These FRP tubes must withstand cyclic compressive loads, in a vacuum environment, at temperatures ranging from cryogenic (1.8 K) to ambient (295 K). The Materials Reliability Division of the National Institute of Standards and Technology (NIST) was contracted to assess the viability of the proposed tube design (Figure 1). Towards such an assessment, NIST performed full scale thermal and mechanical qualification tests of prototype composite support struts.

As a precursor to the full scale tests, a 4.4 MN capacity servo-hydraulic test machine was modified for testing at cryogenic temperatures. Because of the uniqueness of this facility, the details of the cryostat design are presented in the first part of this report. Additional details pertaining to instrumentation are also presented in the same section of the report.

The test program divides into three distinct areas:

(1)   Ultimate compressive strength tests of short specimens.

(2)   Ultimate compressive strength tests of full scale specimens.

(3)   Compressive fatigue tests of full scale specimens.

The experimental results for each of the above tests are discussed in the final section of the report. Additional details are presented on the failure analysis for each type of test, especially for those tests where failure originated with the aluminum end fittings of the tube.

3.0 MECHANICAL TESTING: FACILITIES AND INSTRUMENTATION

3.1 Facility Development

Full scale mechanical qualification tests of the coil support struts were needed for design optimization, fitness for service, and safety. Two types of full scale qualification tests were desired: ultimate compressive strength tests and compressive cyclic fatigue tests. The tests required mechanical loading (to loads in excess of 3000 kN) of the composite tube and an imposed thermal gradient (4 to 295 K) over the length of the tube. To meet these specifications we developed a mechanical test cryostat for a 4.4 MN capacity servo-hydraulic test machine (Figure 2).

The cryostat design was driven by thermal specifications, load capacity, and the size constraints of the test machine. The specimen would be tested between two compression platens at extremely different temperatures. One platen was maintained at room temperature while the other was cooled to extremely low temperatures using liquid helium. The cold platen represents the superconducting coil operating at 1.8 K and the warm platen represents the ambient temperature support trench that the struts are anchored to. In service, each coil support strut thermally loads the 1.8 K coil. To minimize this thermal load, the struts are equipped with liquid nitrogen thermal intercepts at a strategic position along the length of the strut. To best simulate the service environment, the test specimen and test fixture were also equipped with a liquid nitrogen intercept at the appropriate location. The specimen would cool in vacuum by thermal contact conductance with the platens and thermal intercept before testing.

Since the specimen is long (2 m) and one end needed to be at liquid helium temperature (4 K), the cryostat was designed to have the cold end isolated deep in the bottom of a closed bottom super-insulated Dewar. This dictated that a vertical thermal gradient be set up in the test machine with the warm end at the top, thermally anchored to the test machine's heavy framework. This allowed the warm end temperature to be controlled naturally as in the actual application.

The cooling of the lower platen had to be considered carefully from the standpoint of feasibility and cost. The system (cooling and structural) had to be designed efficiently due to the cost of the expendable liquid helium coolant. As in many other design problems, there were material and design selection trade-offs. The conflict was that a 4.4 MN capacity load frame needed to be sized for minimal conductive heat loss and mass. The cooling system for the lower platen (a liquid helium flow heat exchanger) needed to cool this large mass and equilibrate the constant conductive heat losses.

The structure was designed with the lower platen suspended in the Dewar by a four-post cage. The lower platen was efficiently sized to react the bending stress at the 4.4 MN maximum load. The four-post cage also had to react to this load in tension while supplying a direct conduction path to the platen. The lower (cold) platen was a 100 mm thick by 533 mm diameter maraging steel disc with four 60 mm diameter holes for mounting. Four 60 mm diameter titanium rods were used to mount the platen and to transfer the load from the platen to an

3

upper reaction plate. Titanium was used because of its high strength-to-weight ratio and low thermal conductivity. Maraging steel was used for the platen because its high strength allowed for minimal sizing of the part that needed to be cooled with liquid helium. Another reason for selecting maraging steel was the need to solder the copper tube heat exchanger directly to it.

With the optimum physical size of the load frame defined, the cooling system could now be designed. Since the actual support struts in a vacuum are cooled mainly by conduction, the system was designed to cool the specimen by conduction. The cryostat was designed with the specimen and load frame in a vacuum chamber. Liquid helium (4 K) and liquid nitrogen (76 K) flowed through tubing that kept them isolated from the test chamber vacuum space. The liquid cryogens flowed through double-walled, vacuum-insulated plumbing lines until they reached the temperature station that they were supposed to cool (liquid helium at the lower platen and liquid nitrogen at the thermal intercept). Then single-walled copper tubing was used as a heat exchanger. For the lower platen this single-walled copper tubing was soldered directly to the bottom and the circumference of the maraging steel disc. This allowed cooling of the platen by conduction from the convectively cooled copper tubing. The liquid nitrogen thermal intercept was a large copper ring with the single-walled copper tubing soldered to it. This ring was thermally anchored to both the specimen and fixture with copper straps and copper braided cable respectively. Thus, the copper ring, the specimen, and the fixture were cooled by conduction from the convectively cooled copper tubing. The exhaust plumbing for both heat exchangers brought the boiled gases to the outside atmosphere.

The liquid nitrogen thermal intercept was simple compared to the liquid helium cooling system. This was due to a number of factors: the ease with which liquid nitrogen can be handled, the lower thermal load it was required to handle, and the relatively low cost compared to that of liquid helium. For this reason, the liquid helium cooling system is described in more detail.

The liquid helium was responsible for cooling the mass of the lower platen and for equilibrating the heat input from the four titanium support rods. The liquid helium was supplied to the copper tube heat exchanger in 5 mm diameter vacuum-jacketed tubing. A 1.0 l/min liquid helium flow rate was assumed; then, fluid mechanics and heat transfer equations were used to design the heat exchanger. The objective was to have as much length of tubing as possible soldered directly to the platen. The tube diameter was increased ~3 mm, for every 6 m of length, for flow efficiency. The length of copper tubing used to make the liquid helium heat exchanger was ~24 m, starting with an ~5 mm diameter and exhausting through a ~16 mm diameter tube.

The discussion of the facility development has focused on the cryostat internal construction. Two other important areas of the design are the external load frame construction and the accommodations for vacuum sealing.

The configuration of the servo-hydraulic test machine differs from the test machines we normally use for cryogenic mechanical testing. The hydraulic actuator of the 4.4 MN capacity machine is located at the base of the machine while the normal servo-hydraulic machine used for cryogenic tests has a

crosshead-mounted actuator. Normally, cryogenic tests are done in a closed-bottom Dewar and the load frame reacts the load against the upper crosshead.

Using a closed-bottom Dewar necessitated building an external load frame. The frame consisted of two large reaction plates held apart by four long (3 m) columns on the corners. The lower reaction plate (normally the lower platen of the test machine) was mounted to the actuator. The four long columns were mounted vertically on the outside corners on the top of the lower reaction plate. The upper reaction plate was mounted on top of the four columns. The upper plate was machined with a clearance hole (170 mm diameter) in the center to allow a 150 mm diameter push rod to pass through. This rod (chromium AISI 304) is a compressive push rod that rigidly mounts the upper (warm) platen, located inside the cryostat, to the test machine's crosshead, outside the cryostat. The upper reaction plate also has a four hole pattern for mounting the four-titanium- post cage containing the lower platen. When the hydraulic actuator is moved, the motion of the lower reaction plate is transmitted by the four columns, to move the upper reaction plate. Since the four titanium posts are also connected to the upper reaction plate, they move the lower platen in unison with the actuator. This large double-cage apparatus moves with the actuator while the compressive push rod and upper platen remain stationary. To apply a load the test specimen must be in place on top of the lower platen. The specimen is compressed when the actuator is moved up and the specimen contacts the stationary upper platen.

The next area to be discussed is some of the design details of the vacuum chamber. Since the cryostat was designed to fit in a closed bottom, open mouth Dewar all of the vacuum seals were at the top of the Dewar. The Dewar was constructed with an O-ring flange top with a mounting bolt pattern. The upper reaction plate of the test fixture acted as the top of the Dewar that needed to be sealed. With the cryostat assembled, the Dewar fit inside of the four-column external load frame.

To accommodate the necessary access ports for the internal vacuum chamber, an adapter plate was machined to fit between the Dewar flange and the upper reaction plate. Vacuum feed-through ports were needed for the cryogenic plumbing lines and instrumentation lead wires. The adapter plate was machined from a canvas-phenolic composite material and was O-ring sealed when mounted to the upper reaction plate. The necessary plumbing inlet and exhaust ports were epoxy-potted into machined grooves in the composite plate. Pipe-threaded access ports were machined to accommodate commercial instrumentation vacuum feed-throughs. A bolt stud pattern was used to seal the Dewar flange to the composite adapter plate.

The compressive push rod (150 mm diameter chromium-plated AISI 304) was sealed where it entered the vacuum chamber, at the top of the upper reaction plate, using an O-ring flange specifically designed for the dynamic motion of the push rod.

The Dewar was equipped with a vacuum pump port into the inner chamber. A large (760 l/min) mechanical vacuum pump was used to evacuate the chamber. Lower vacuum pressure than the pump could attain was assumed possible due to cryo-pumping from the liquid helium cooled components inside of the test chamber.

3.2 Instrumentation

This section details the various types of instrumentation used for all tests. The physical data to be recorded were load, displacement, temperature, and vacuum pressure. The data were recorded with a computer data acquisition system and an analog x-y chart recorder. Since all tests were basically compression tests of a tube, one requirement common to all tests was a record of load versus displacement. The load was measured using the test machine's load cell. Other data measurements varied and are described for individual tests.

Three alternative methods of displacement measurement were used: localized specimen strain measurement using strain gages bonded directly on the specimen, overall specimen displacement measurement using LVDT's (linear variable differential transformer) from specimen end-to-end, and as a backup method, the test machine's stroke displacement was also measured with an LVDT. Strain gages were bonded directly to specimens 005, 005-1, 006-1, and 008. Each specimen had four strain gages longitudinally mounted and radially spaced 90° apart. For short specimens, the gages were located half-way along the length. For long specimens, the gages were located ~500 mm from the top (warm) end fitting. The strain gage signals were conditioned with a commercial strain indicator and a three leadwire, quarter bridge configuration was used. The leadwires were soldered to the leadwire vacuum feed-through port for the long specimen test.

Two LVDT's were used to measure displacement on specimens 005, 005-1, 006-1, and 009. Overall specimen displacement was measured using two LVDT's, radially spaced 180° apart, on opposite sides of the specimen. The core of the LVDT was attached to the upper platen to ensure that it remained warm during testing. An extension rod (6 mm diameter Invar) was attached to the center rod of the LVDT. It extended down the length of the specimen and contacted the top of the lower platen. After the test on specimen 009, one of the LVDT's was damaged, so for the next test on specimen 007, only one LVDT was used. For the two short specimens 005-2 and 006-2, without end fittings, displacement data were obtained from the test machine stroke LVDT.

Temperature data was obtained for all the thermal gradient tests using type-E (chromel/constantan) thermocouples. The specimen and the test fixture were instrumented with thermocouples to monitor the thermal gradient. Each thermocouple bead was securely attached to the specimen or fixture at strategic locations along the length of the apparatus. The thermocouple leadwires were soldered to a thermocouple reference junction/vacuum feed-through port. Shielded copper wire pairs connected each thermocouple reference junction to a 20 channel digital voltmeter. The thermocouples were calibrated in this configuration. The thermocouple data were taken directly from the digital voltmeter into the computer data acquisition system.

The vacuum pressure in the test chamber was monitored continuously with a thermocouple gage and analog readout unit. The system was capable of reading pressures ranging from atmospheric down to 0.133 Pa (1 mTorr).

6

4.0 EXPERIMENTAL RESULTS AND DISCUSSION

In this section we present the details of all tests performed on the composite support struts. Load-versus-displacement records and temperature gradient data are provided for each test. Finally, a short discussion and conclusions are given for each group of tests. Some remarks are also given for the suspected mode of failure for each test.

4.1 Ultimate Compressive Strength: Short Specimens

Four short specimens (two, 0.3 m long and two, 0.6 m long) of the full scale diameter tube were available for testing. They were tested at ambient temperature to obtain some base properties of the prototype tubes. The two shorter tubes (specimens 005-2 and 006-2) were tested without any special end fittings. The ends of the composite tubes were set directly on the compression platens. The 0.6 m long tubes (specimens 005-1 and 006-1) were equipped with aluminum (7075-T6) end fittings. The end fittings, shown in Figure 3, slide onto the ends of the tube and are designed to prevent brooming of the tube ends. If end fittings are not used, the tube fails by brooming and the materials maximum strength is not actually measured. The load-versus-displacement curves for all four tests are shown in Figure 4.

For the short-specimen tests, the cryostat test fixture was not used. The specimens were compressed to failure between platens in the 4.4 MN capacity test machine. A compression swivel platen was attached to one of the test machine's rigid compression platens to ensure axial loading of the test specimen. The load was applied using a ramp function in a displacement control mode. Overall specimen displacement was measured using LVDT's from platen to platen. Additional strain measurements used strain gages bonded to the specimen. Load versus displacement curves (LVDT) were plotted on an x-y recorder.

Specimen 005-1

The undamaged portion of specimen 005 from the full scale tests was cut off at 0.66 m (26 in). The end fitting from the warm end of the tube in the full scale test was intact and not removed. A new end fitting was machined for use on the other end of the short specimen. This end fitting was pressed on the short tube and potted in epoxy under a 445 kN (100 kips) compressive load.

The specimen was tested at 295 K in a 4.4 MN (1000 kips) servohydraulic test machine. The specimen failed at a maximum compressive load of 1.6 MN (369 kips). The specimen failed in primarily a shell-buckling mode, but a longitudinal crack running the length of the specimen was found in post-mortem analysis. One end fitting had an exterior surface crack, radially oriented, about 150 mm (6 in) long.

Specimen 006-1

Full scale specimen 006 failed during the installation of the end fittings as described later in this report. The damaged ends of specimen 006 were cut off

7

and provided a 0.58 m (23 in) specimen without end fittings. New end fittings were then installed before testing.

The specimen failed at a maximum compressive load of 1.7 MN (384 kips) in the 4.4 MN (1000 kips) test machine. The primary failure mode was shell buckling which was also the failure mode of specimen 005-1. The shell buckling was preceded by a large longitudinal crack which initiated at the rigid aluminum end fitting and propagated the length of the specimen.

The aluminum end fitting exhibited premature failure at approximately half the maximum load. The end fitting failure was characterized by radial cracking on the exterior surface. The location of the cracking showed that the cracks initiated at the bottom of the internal groove. The cracks were 75 to 100 mm (3 to 4 in) long in about four places.

Specimen 005-2

An additional 0.31 m (12 in) specimen was available from the undamaged portion of specimen 005. This short tube was tested with no end fittings to gain additional data on the material's ultimate compressive strength. The test was performed under isothermal conditions at room temperature (295 K). The specimen failed at a maximum compressive load of 2.4 MN (536 kips). The specimen failed catastrophically by brooming on one end.

Specimen 006-2

This 0.36 m (14 in) specimen was removed from the undamaged portion of full-scale specimen 006. Similar to specimen 005-2, this specimen was tested under isothermal conditions at room temperature (295 K). The specimen failed at a maximum compressive load of 2.4 MN (538 kips), nearly identical to the failure load of specimen 005-2. The mode of failure was again brooming from one end of the specimen.

Summary of Results

The results of the two tests without end fittings (specimens 005-2 and 006-2) are almost identical and are shown in Table 1. Both specimens failed at approximately 2.4 MN (540 kips) compressive load and both failed due to brooming on one end. The average cross-sectional area of the specimens was 64 cm^2 (10 in^2), and the average ultimate strength was 375 MPa (54 ksi).

The other two tests (specimens 005-1 and 006-1) failed at loads of 1.6 MN (369 kips) and 1.7 MN (384 kips) giving an average ultimate strength of 262 MPa (38 ksi). The failure mode for these two tests was shell buckling, but both tubes had longitudinal cracks emanating from one end (see Figure 5). The end fittings also exhibited initial signs of failure on both tests. Circumferential cracks on the exterior surface of the end fitting (relative to the base of the internal machined groove) were observed (see Figure 6).

8

Conclusions

The short specimens without end fittings failed at higher stresses than the longer specimens with end fittings. It cannot be concluded that end fittings were detrimental to the tube strength since there was also the variable of specimen length. The decrease in tube strength is due to the change in mode of failure from end brooming to shell buckling. The initial signs of failure of the end fittings indicate a problem area where large stresses are too close to a geometric stress concentration (the root radius at the base of the machined groove).

4.2 Ultimate Compressive Strength: Long Specimens

One full scale cryogenic test (specimen 009) is discussed in detail and another unsuccessful full scale test (specimen 005) is briefly discussed. Both specimens were full length (~2 m) and were tested in the 4.4 MN cryogenic test machine. The specimens were equipped with the aluminum end fittings described previously. The cryogenic test of specimen 009 was a controlled thermal gradient compression test, using liquid nitrogen (76 K) for cooling. The test of specimen 005 preceded this test and was intended to be an ambient temperature, full scale compression test as well as a proof test of the cryostat load fixture; however, this specimen was inadvertently heated during testing, which caused premature failure.

Specimen 005

Specimen 005 was shortened to 1.61 m (63.5 in) from its original 1.98 m (78.0 in) length to properly scale the buckling conditions from cryogenic to room temperature. Also, a small portion of the tapered end of the tube was removed because of some visible delaminations. The end fittings used for this ultimate compression strength test were fabricated from 7075 aluminum and did not use the lead pad. The end fittings were press-fitted to the specimen, potted in epoxy, and subjected to a 4.4 kN (100 kips) compressive load during curing of the epoxy.

The test on specimen 005 was a test of the material as well as a learning exercise on the assembly and operation of the 4.4 MN cryostat. The test set-up was identical to a full scale cryogenic test without the super-insulated Dewar. This made it possible to view the specimen during testing. In hopes of visually observing specimen damage upon loading, two 100 W light fixtures were installed inside the tube. The lights were turned on when the specimen was initially loaded, then after a ~30 min instrumentation and fixture proofing procedure, the test was started. The specimen was ramp loaded and failed prematurely at 445 kN (100 kips) by column buckling near the midpoint (approximate location of the lights). Immediately after failure, the buckled specimen was examined and found to be warm. The external surface of the specimen was approximately ~25°C above room temperature. Specimen creep was observed as the load was applied, but the temperature rise was not observed until after the tube failed.

Specimen 006

This was originally to be a full scale room-temperature test with lead-pad end fittings. The full length specimen was cut to 1.61 m (63.5 in), removing

9

material from the cold end (straight section) to reduce the critical column buckling stress that is the dominating failure criteria for warm tests.

This test was never run because a longitudinal crack initiated when the end fittings were pressed on the tube. This failure is probably due to the interference fit between the inside diameter of the tube and the inside diameter of the end fitting groove. The larger diameter of the groove in the aluminum end fitting caused a large diametral strain and hoop stress on the tube that caused initiation of the longitudinal crack.

Specimen 009

Specimen 009 was a full scale test conducted in a thermal gradient. The specimen was equipped with rigid end fittings which necessitated the use of a swivel platen to ensure axial loading of the specimen. Liquid nitrogen (76 K) was used to cool the lower two-thirds of the test fixture and specimen. The goal was to test a full length (2 m) tube with an imposed cryogenic thermal gradient and to verify the cryostat thermal efficiency before liquid helium (4 K) tests. Some problems, such as cryostat vacuum leaks and specimen thermal intercept inefficiency, were noted for future repair.

With liquid nitrogen, the lowest temperature attainable for the thermal gradient is 76 K. The ideal conditions would be isothermal for the lower two-thirds of the specimen at 76 K, then a gradient from 76 K to ambient (295 K) over the upper one-third of specimen length. This ideal gradient was not obtained due to time constraints and the low thermal conductivity of the specimen. The actual gradient attained on the specimen is shown schematically in Figure 7 and ranged from 115 to 278 K.

The specimen was loaded in compression using manual displacement control. The load was applied in 2 kN (450 lb) increments. At each load step, the test was interrupted for data acquisition and all transducers were scanned. The compressive load versus displacement curve is shown in Figure 8. The specimen failed with a loud acoustic emission at 3.34 MN (752 kips).

Summary of Results

Specimen 009 failed in the mid-region, where the liquid nitrogen thermal intercept was attached (Figure 9). At this location, several factors could influence the stress field in the material. The mechanical attachment of the thermal intercept (Figure 10) could increase the localized stress on the specimen since it confines diametral strain when the tube is compressed. This is also the location along the length of the specimen where the specimen changes from a constant cross-sectional area (see Figure 1) to an increasing outside diameter and increasing cross-sectional area.

The ultimate compressive strength of specimen 009 was 518 MPa (75 ksi). The temperature in the region of fracture was 140 K. The elastic modulus calculated from the load-displacement curve was 45 GPa (6.5 Msi). Total strain to failure was 0.0135.

10

The specimen failed catastrophically by a combination of failure modes: shell buckling, column buckling, and longitudinal cracking. Column buckling is indicated by the midlength fracture and the angle at which the specimen came to rest after the failure event. Shell buckling is inferred from the appearance of the fracture area: both halves of the specimen are broomed, splayed, and pushed together (Figure 9). Both end fittings exhibited the initial signs of failure described for the previous short specimen tests: circumferential cracking on the exterior surface relative to the base of the internal machined groove (Figure 6).

Conclusions

The full scale, ultimate compressive strength test on specimen 009 was successful in characterizing the mechanical performance of the FRP tube subjected to a thermal gradient. The failure stress (518 MPa) was slightly lower than expected (620 MPa). The location of the failure is a potential problem that needs further design evaluation. It is also important that the specimen failed in a cold (140 K) region. Further down the specimen (Figure 7), the temperature was higher (190 K) and the stress was equivalent (518 MPa). The end fittings again exhibited cracking which possibly induced premature failure of the FRP tubes.

4.3   Fatigue Tests

Two extreme thermal gradient tests, using liquid helium cooling, are discussed in this section. The first (specimen 007) was a cyclic fatigue test that had multiple failure events before total catastrophic failure at 385 cycles. The second (specimen 008) was a single load cycle test performed with approximately the same environmental and mechanical conditions to help analyze the results of the first test. The two fatigue specimens were fitted with self-aligning end fittings. The difference in design between the two types of end fittings is shown in Figure 11.

Specimen 007

Since the full scale test of specimen 009 was successful, we were able to return to the original test plan for the remaining two specimens. The original test plan called for fatigue tests to be performed with the 4 to 295 K thermal gradient along the length of the test specimen. The test plan specified that the tube be cyclically loaded in compression to approximately 310 MPa (45 ksi) at the warm end for 22 000 cycles. The 310 MPa (45 ksi) stress is based on 1.5 times the operating design stress of 207 MPa (30 ksi). The actual fatigue conditions were cyclic loading to 276 MPa (40 ksi) using a sawtooth waveform with a stress ratio R ratio of 0.1 and a frequency of 0.25 Hz (Figure 12). The slightly lower maximum stress was used since the ultimate strength of the material was 20 percent lower than expected.

The end fittings were epoxied into the specimen under a 445 kN (100 kips) compressive load. The specimen was wrapped with 50 mm (2 in) wide aluminized tape on the outside diameter to provide a layer of thermal radiation insulation. The inside of the tube was filled with crumpled, aluminized Mylar film, also for thermal radiation insulation. With the tube in the fixture, the whole fixture

11

was wrapped with aluminized Mylar sheet, another thermal radiation barrier. The thermal gradient measured just before testing is shown in Figure 13.

Due to the complexity of this full scale test, the first load cycle was controlled manually. The load was applied with the machine in displacement control in approximately 4.4 kN (1000 lb) increments. The load-versus-displacement curve, shown in Figure 14, was linear to 1.2 MN (282 kips), when a loud noise occurred. The specimen load dropped to 1.0 MN (230 kips), and the load- versus-displacement curve shifted an amount that indicated 3.5 mm (0.14 in) of platen-to-platen closing. The specimen was then manually unloaded to 0.76 MN (170 kips) and had the same linear elastic slope as before the noise. The specimen was then reloaded to 1.0 MN (230 kips) where the manual incremental step loading was restarted. The desired maximum fatigue load of 1.8 MN (400 kips) was reached without incident. The specimen was unloaded to the minimum fatigue load of 0.18 MN (40 kips) and the test machine was switched to load control in preparation for the computer controlled fatigue waveform.

The specimen was loaded with a triangular waveform, in load control, at a frequency of 0.25 Hz as shown in Figure 12. The fatigue cycle continued for 385 cycles until another loud noise occurred. The fatigue cycle was stopped and again the specimen was still able to sustain a load. The specimen was reloaded manually from zero load and the load-versus-displacement curve was monitored. The curve again had the same linear elastic slope but had shifted 5.3 mm (0.21 in) from the initial loading curve (cycle number 1). This manual reloading cycle was curiously normal until another loud noise at 1.7 MN (380 kips) signaled total catastrophic failure of the specimen: no load could be sustained with further displacement of the actuator.

The specimen failed at the bottom (or the cold end) as shown in Figure 15. The failure mode appeared to be shell buckling. The failed area covered about 300 mm (1 ft) of length starting 25 mm (1 in) from the bottom end of the specimen. The specimen also contained numerous longitudinal cracks emanating from the bottom end of the specimen. Examination of the longitudinal cracks revealed approximately ten, 300 to 900 mm (2 to 3 ft) long cracks and many short 50 to 150 mm (2 to 6 in) cracks spaced approximately 13 mm (0.5 in) apart.

The longitudinal cracking of the specimen on the cold end effectively changed the specimen's geometry from a tubular cross-section into a series of independent columns. The ultimate failure of the specimen was local buckling of the slender columns.

Both end fittings on the specimen showed signs of failure as shown in Figure 16. The lower (cold) end fitting completely fractured into multiple pieces as shown in Figure 15. The band of material on the outside of the machined groove in the lower end fitting fractured at the base of the groove and was no longer in place to function as designed. This may be the reason for the initiation of longitudinal cracks in the specimen. The upper (warm) end fitting had radial cracks visible on the outside surface but had not completely fractured as in the lower end fitting. Another problem for both end fittings was the area machined for placement of the lead pad. Both end fittings fractured between a fillet in this machined area and the free surface. The fracture path was slightly different for each end fitting as shown in Figures 15 and 16.

12

Specimen 008

Due to the uncertainty of the dominating failure mode on the previous test, we performed an interrupted test on the final specimen. The plan was to terminate the test after the first sign of failure (a loud noise or anomalous load and
strain behavior). The thermal conditions of the previous test were duplicated as closely as possible.

The full length (2 m) specimen was fit with the self-aligning end fittings. The cold end fitting fit the specimen well and was not epoxied on. The warm end fitting fit well on the inside diameter of the tube, but had excessive clearance between the outside diameter and the groove. There was an approximately 1.3 mm (0.05 in) gap around the outside of the tube that we filled with fiber-glass cloth and epoxy. It was necessary to fill this void to give the specimen side support on the end. The epoxy cured with the specimen under a 44 kN (10 kips) compressive load. This specimen was not wrapped with aluminized tape, but the test fixture was skirted with aluminized Mylar sheet for thermal radiation insulation. The inside of the tube was filled with crumpled aluminized Mylar sheet also for thermal radiation insulation.

The specimen was placed in the test fixture at ambient temperature. The fixture was sealed and the vacuum roughing pump and liquid nitrogen cooling were started simultaneously. Liquid nitrogen was used to cool the three cooling coils for approximately 75 h at an average of 19 1/h. The rough vacuum during this interval was ~27 Pa (~200 mTorr).

As in previous tests the specimen temperature was higher than the fixture temperature. After 75 h of phase I (liquid nitrogen only) cooling the lower platen of the test fixture was 85 K, the lower end fitting was 91 K and 25 mm (1 in) above the lower end fitting the temperature of the specimen was 137 K. At this point, phase II of the cooling was started. Two 500-1 Dewars of liquid helium were connected to the two 4 K cooling circuits. Approximately 10 to 15 min after the start of liquid helium flow, the test chamber vacuum pressure dropped from 27 Pa (200 mTorr) to 1.3 Pa (10 mTorr). During phase II liquid nitrogen flow was maintained in the 76 K thermal intercept.

The liquid helium/liquid nitrogen cooling of the test apparatus was conducted for approximately 12 h before the start of the compressive test. The respective flow rates for the liquid helium/liquid nitrogen cooling were 48 1/h and 8 1/h.

After 12 h in phase II cooling, the lower platen and the lower end fitting temperatures were both 35 K while 25 mm (1 in) above the end fitting, the specimen temperature was 83 K. At the intermediate liquid nitrogen thermal intercept the specimen temperature was 100 K. The thermal gradient measured just before testing is shown schematically in Figure 13.

The specimen was loaded manually in displacement control. The loading was suspended every 8.9 kN (2 kips) and all transducers were scanned. The resulting load-versus-displacement curve, shown in Figure 14, was linear up to point A, where a loud acoustic emission was heard. The load at this point was 1.16 MN

13

(260 kips) and it dropped instantly to 0.93 MN (210 kips). The load-versus-displacement curve shifted to the right by an amount that indicated approximately 2 mm (0.08 in) of platen-to-platen closing. This load drop, curve shift, and acoustic emission indicated some type of failure so we stopped the test to inspect the specimen. The specimen unloading curve was linear and parallel to the original loading curve.

The test specimen remained intact but the lower (cold) end fitting was completely fractured into multiple pieces. The failure of the lower end fitting was essentially identical to the failure of the lower end fitting on specimen 007. The band of material on the outside of the machined groove completely fractured at the base of the groove. There was also complete fracture of the end fitting, in the area recessed for the lead pad, identical to previous failures of the lower end fitting.

The specimen exhibited the start of numerous longitudinal cracks emanating from the bottom of the specimen. The 50 to 100 mm (2 to 4 in) long cracks were spaced approximately every 13 mm (0.5 in) about the circumference of the specimen.

The load at which this end fitting failed was within 8 percent of the load at the first failure event in the previous test. This coincidence of load and the similarity of the two failed end fittings leads us to conclude that the first failure event in the previous test also occurred in the lower (cold) end fitting.

Summary of Results

Examination of specimen 007 indicated that the specimen and both end fittings failed. The specimen failed at the cold end as shown in Figures 15 and 16. The end fitting at the cold end had fractured into multiple pieces (Figure 16A) while the warm end fitting fractured into two pieces (Figure 16B).

The single cycle compressive test of specimen 008 caused the cold end fitting to fail. The failure of the end fitting into multiple pieces was essentially identical to the previous failure of the cold end fitting on specimen 007.

Conclusions

The most important conclusion from these tests is that the compressive self-aligning end fittings must be redesigned to develop the full strength of the composite tube. Previous tests performed using the rigid aluminum end fittings alluded to a strength problem. The self-aligning end fittings contain more geometric stress concentrations than the rigid end fitting. This combined with the more brittle behavior of the 7075-T6 aluminum alloy at cold temperatures was detrimental to end fitting performance. Both tests failed on the first load cycle at almost identical stresses (186 ± 8.5 MPa). For specimen 007, it was not possible to verify the cold end fitting failure as the first failure but that conclusion was confirmed by the test of specimen 008.

Since the failure of the cold end fittings prohibited further determination of the composite tube properties, the only other conclusion from the test on

specimen 007 is that the fatigue life of the tube for the documented thermal and mechanical conditions is greater than 385 cycles for the loading conditions described above.

5.0   **SUMMARY AND CONCLUSIONS**

The results of all tests of the FRP support tubes are summarized in Table 1. For each test, the thermal conditions, ultimate load, and failure mode are indicated. We conclude the following:

(1)   The failure stress on the full scale, ultimate compressive strength specimen (specimen 009) was nearly 20 percent lower than expected.

(2)   The end fittings for the tubes present the greatest obstacle to loading the tubes to their ultimate strength.

(3)   The stress concentration of the end fittings is a problem that is magnified with the present design of the self-aligning end fittings.

Table 1: Test result summary sheet.

Specimen No.	Length (m)	Thermal Conditions	End Fitting*	Ult. Load (kN) (kips)		Ult. Stress (MPa) (ksi)		Failure Mode†
005	1.60	320 to 295 K gradient	2	448	100	70	10.0	3
005-1	0.66	295 K, isothermal	2	1641	369	254	36.9	1,4
006-1	0.58	295 K, isothermal	2	1708	384	265	38.4	1,4
006-2	0.35	295 K, isothermal	1	2393	538	371	53.8	2
005-2	0.30	295 K, isothermal	1	2384	536	370	53.6	2
009	2.00	120 to 280 K gradient	2	3345	752	519	75.2	1,3,4
007	2.00	25 to 273 K gradient	3	1284	282	194	28.2	5
008	2.00	35 to 273 K gradient	3	1156	260	179	26.0	5

*End Fitting Notes

(1) no end fittings

(2) ultimate load (rigid) end fittings

(3) self-aligning end fittings

†Failure Mode Notes

(1) longitudinal crack initiated at end

(2) brooming at end

(3) column buckling

(4) shell buckling

(5) end fitting failure

23.7 cm

26.7 cm

0.67 m

Start of taper
(increasing outside
diameter for upper
0.67 m).

2.0 m

1.33 m

0.85 cm

25.4 cm
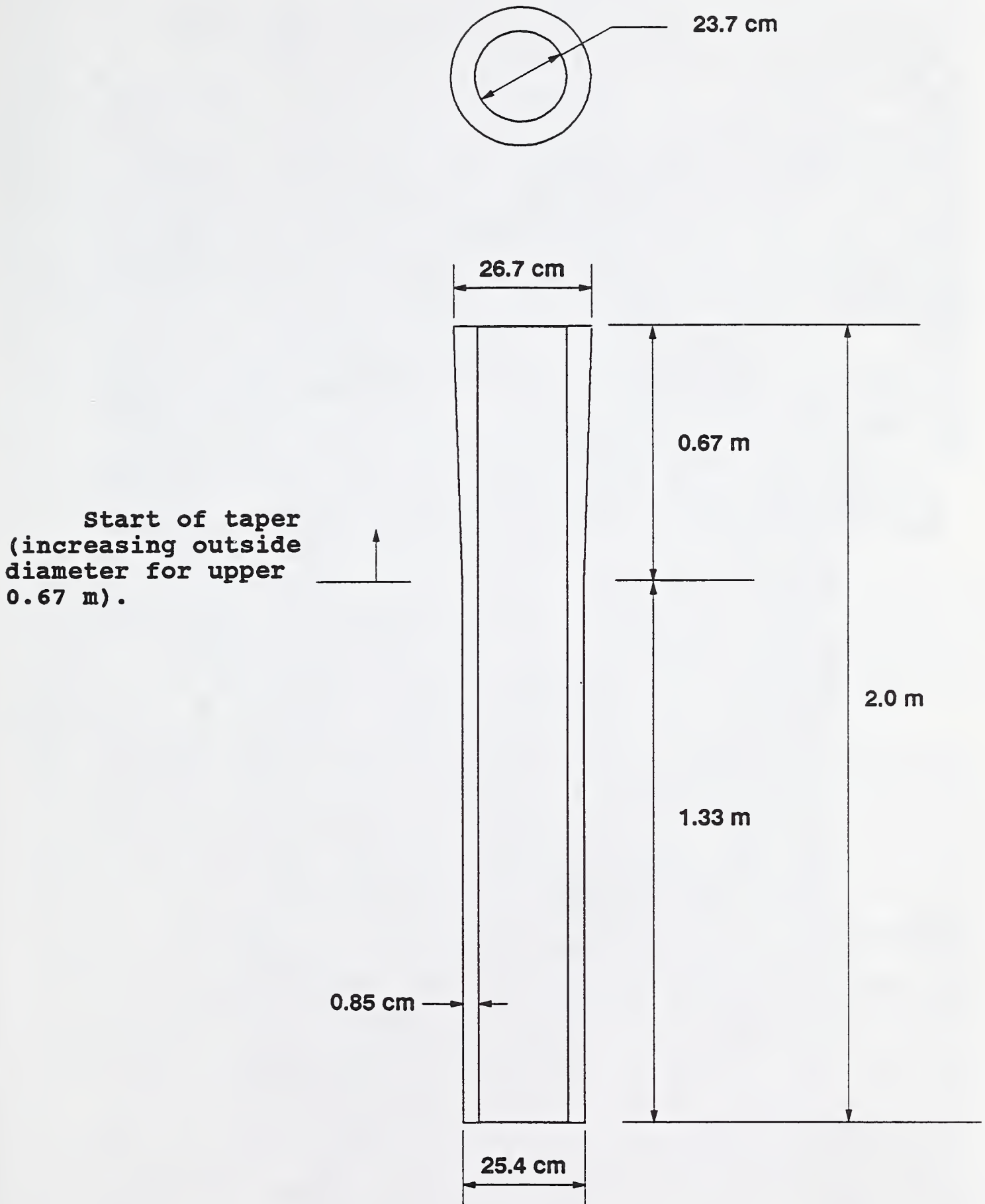
Figure 1. Schematic of composite tube.

17
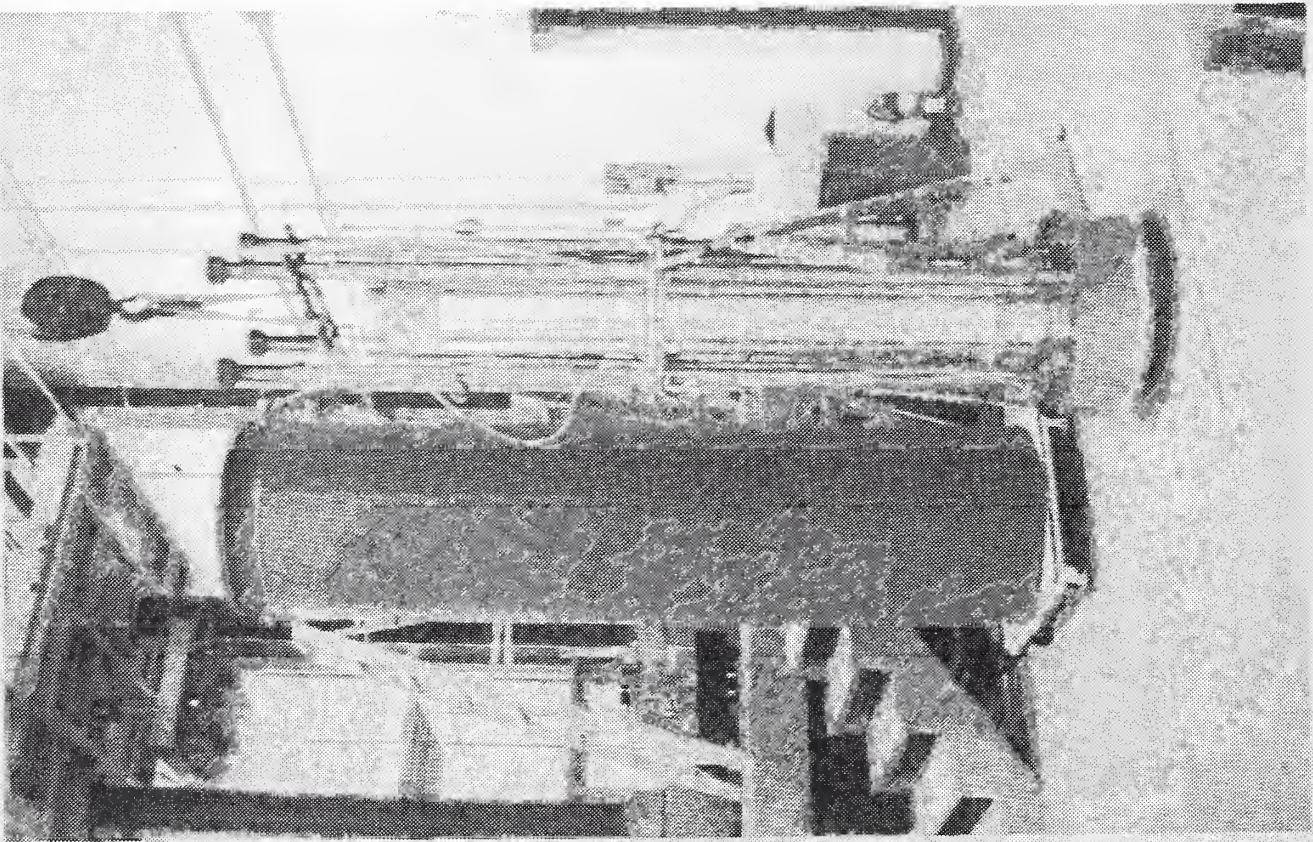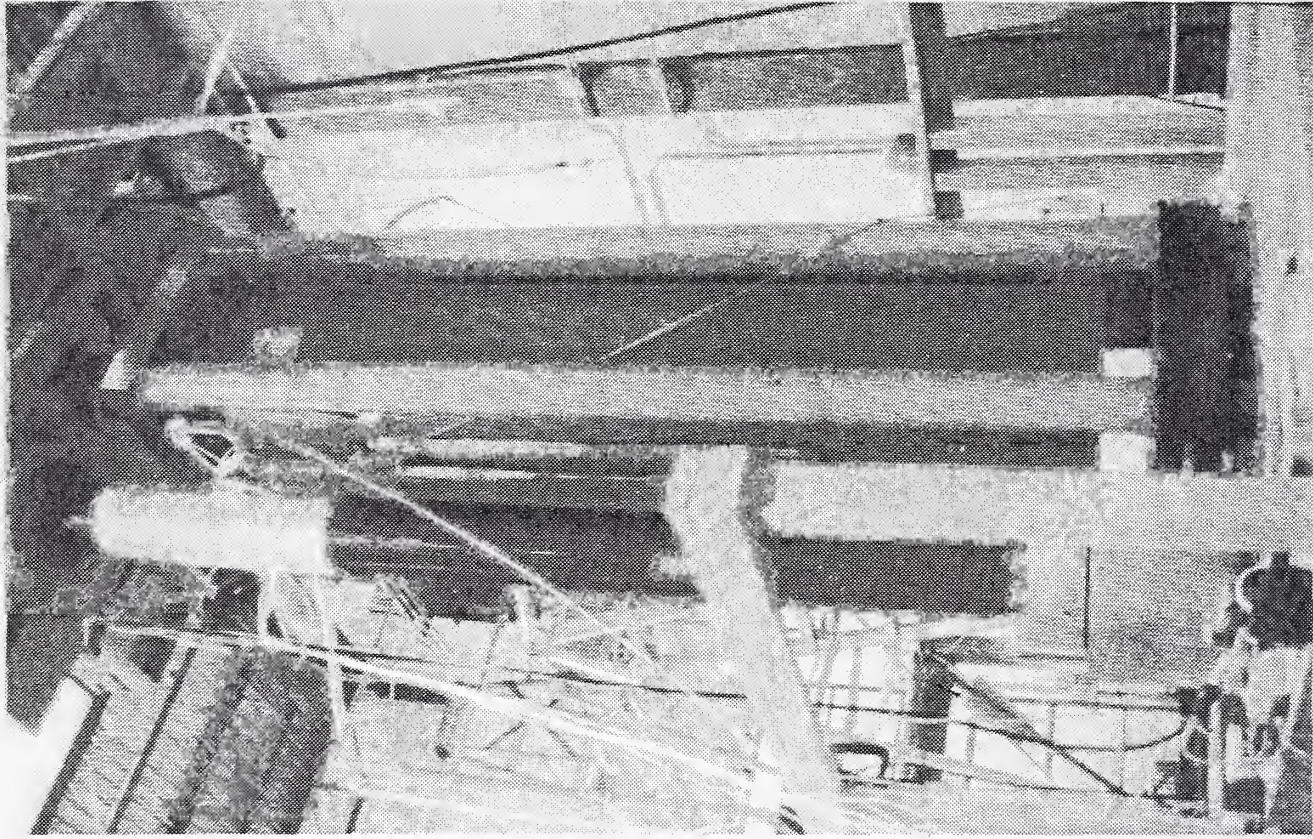
Figure 2. 4.45-MN (1000 kips) test machine and cryostat.
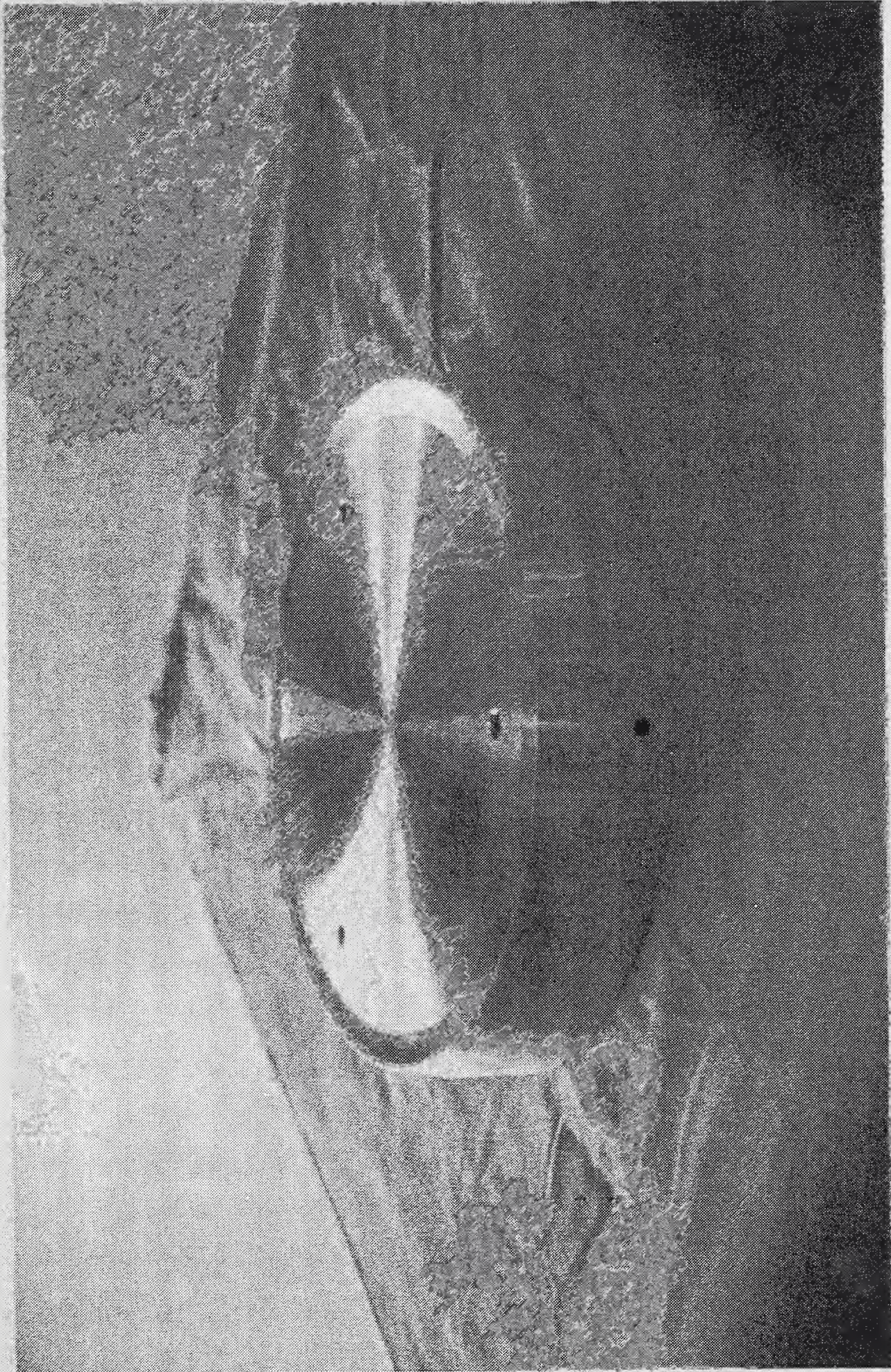
Figure 3. Rigid end fitting (7075 T6 Al)

19
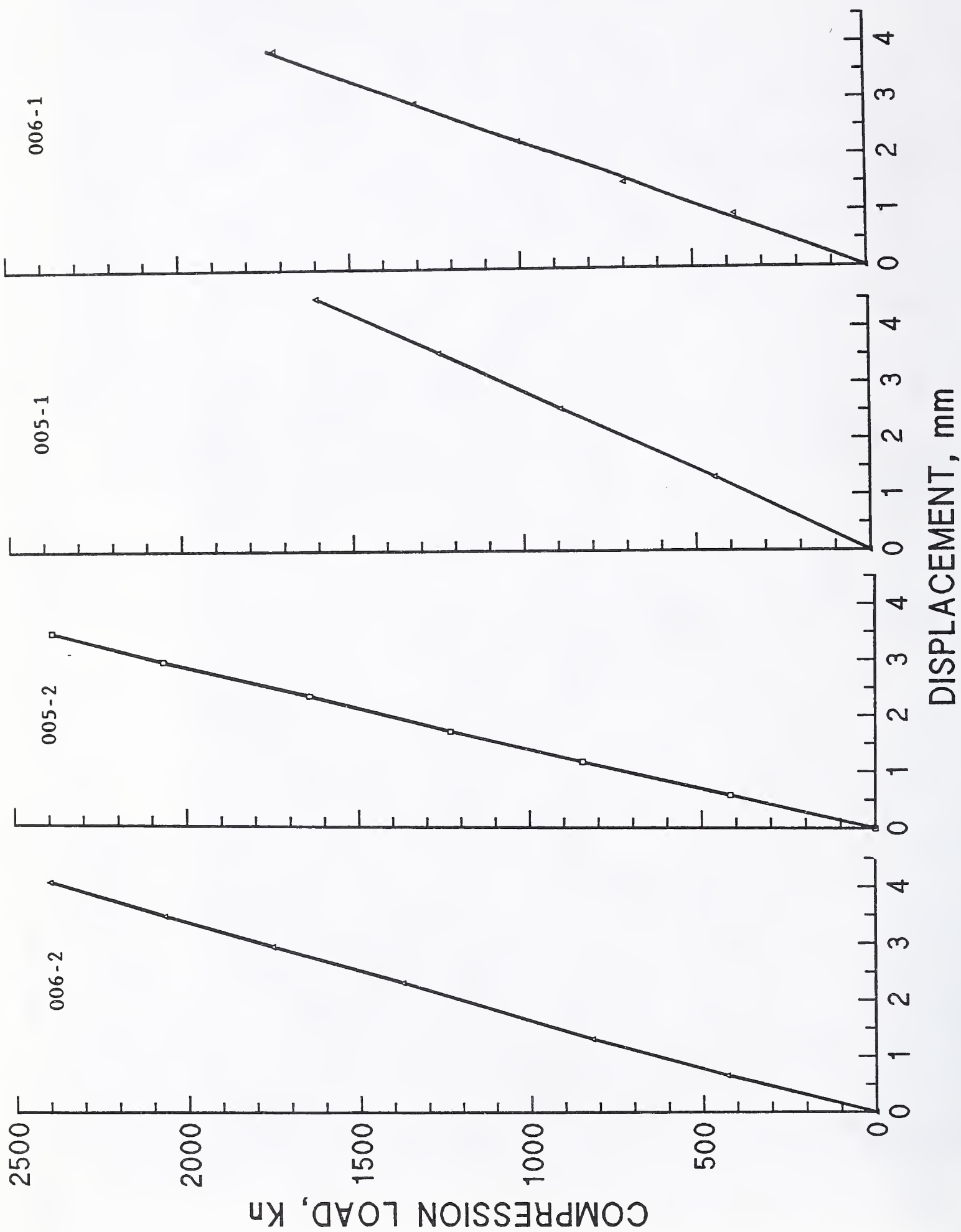
Figure 4. Load-versus-displacement curves for short specimen tests.

20
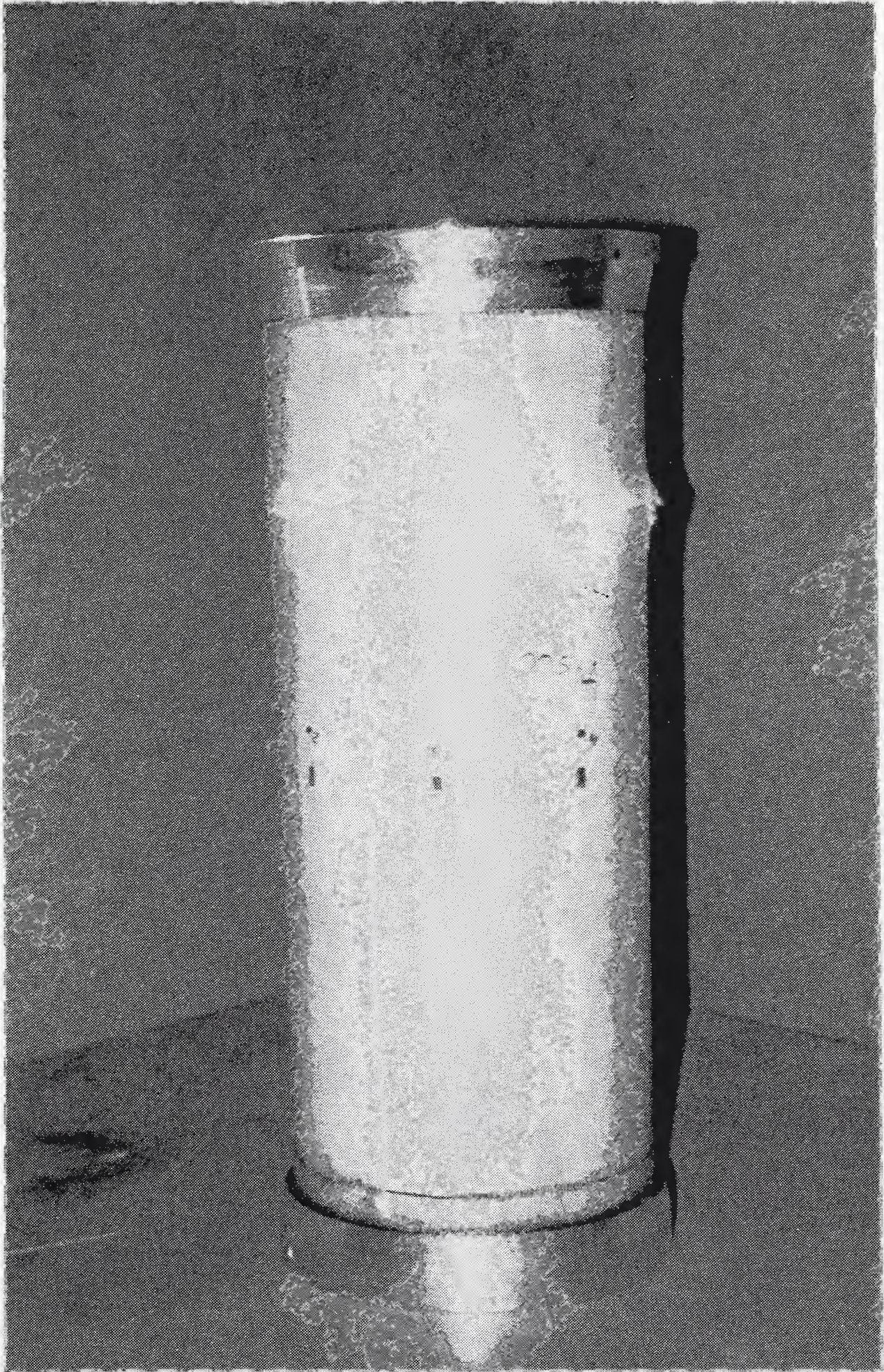
Figure 5.   A failed short specimen with end fittings.
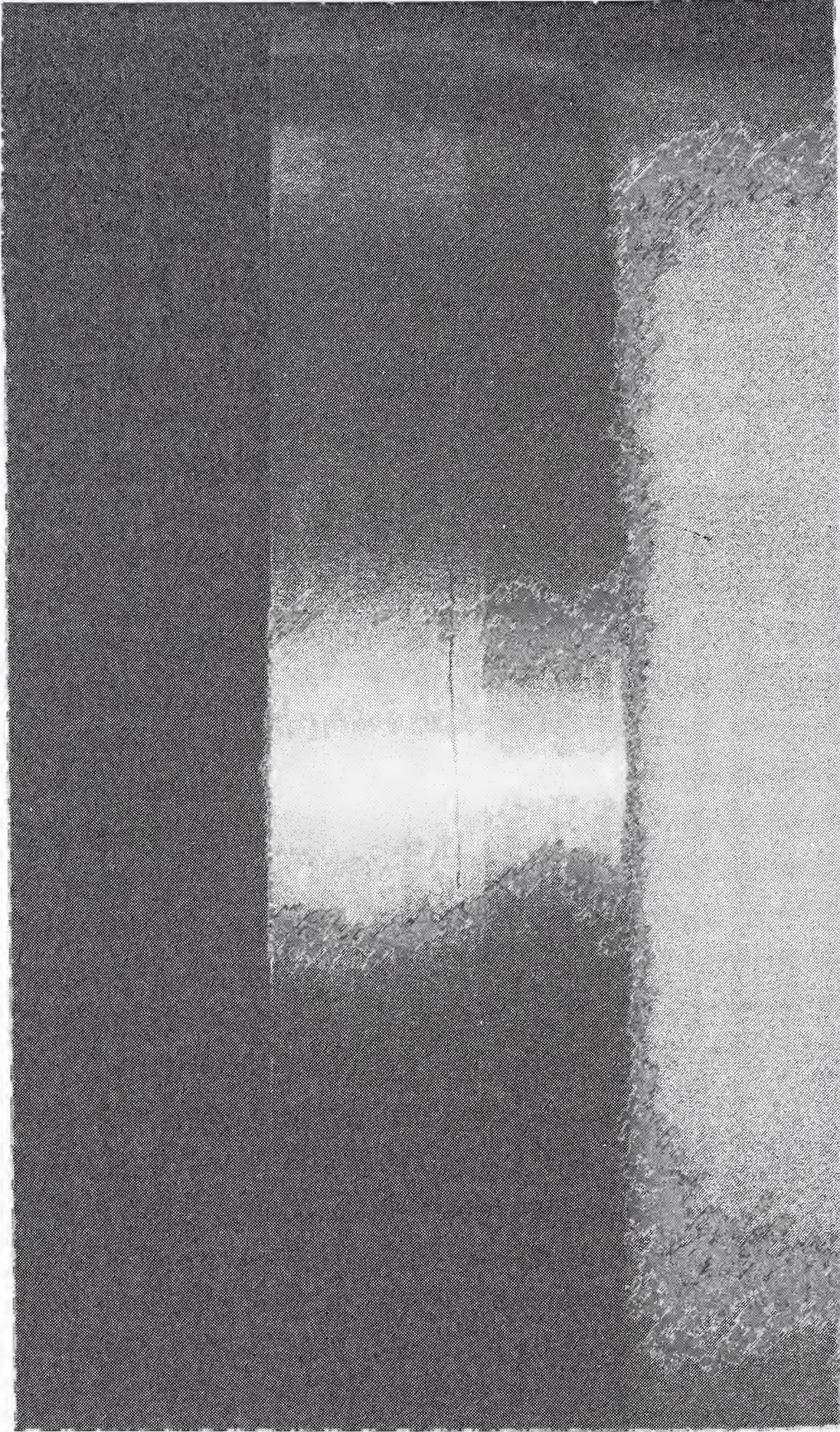
Figure 6. A circumferential crack on surface of end fitting.
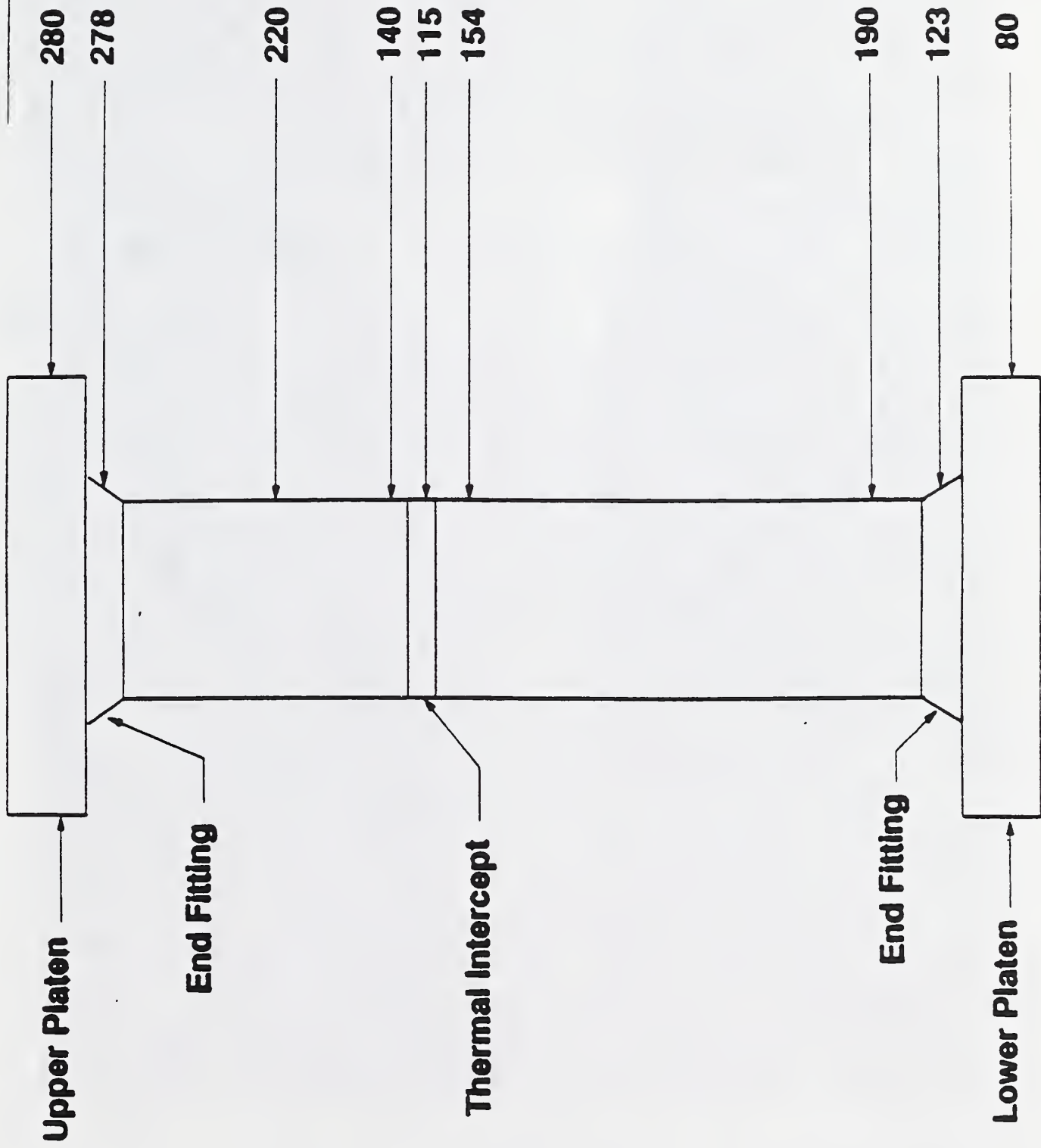
Figure 7.   Schematic for thermal gradient of specimen 009.
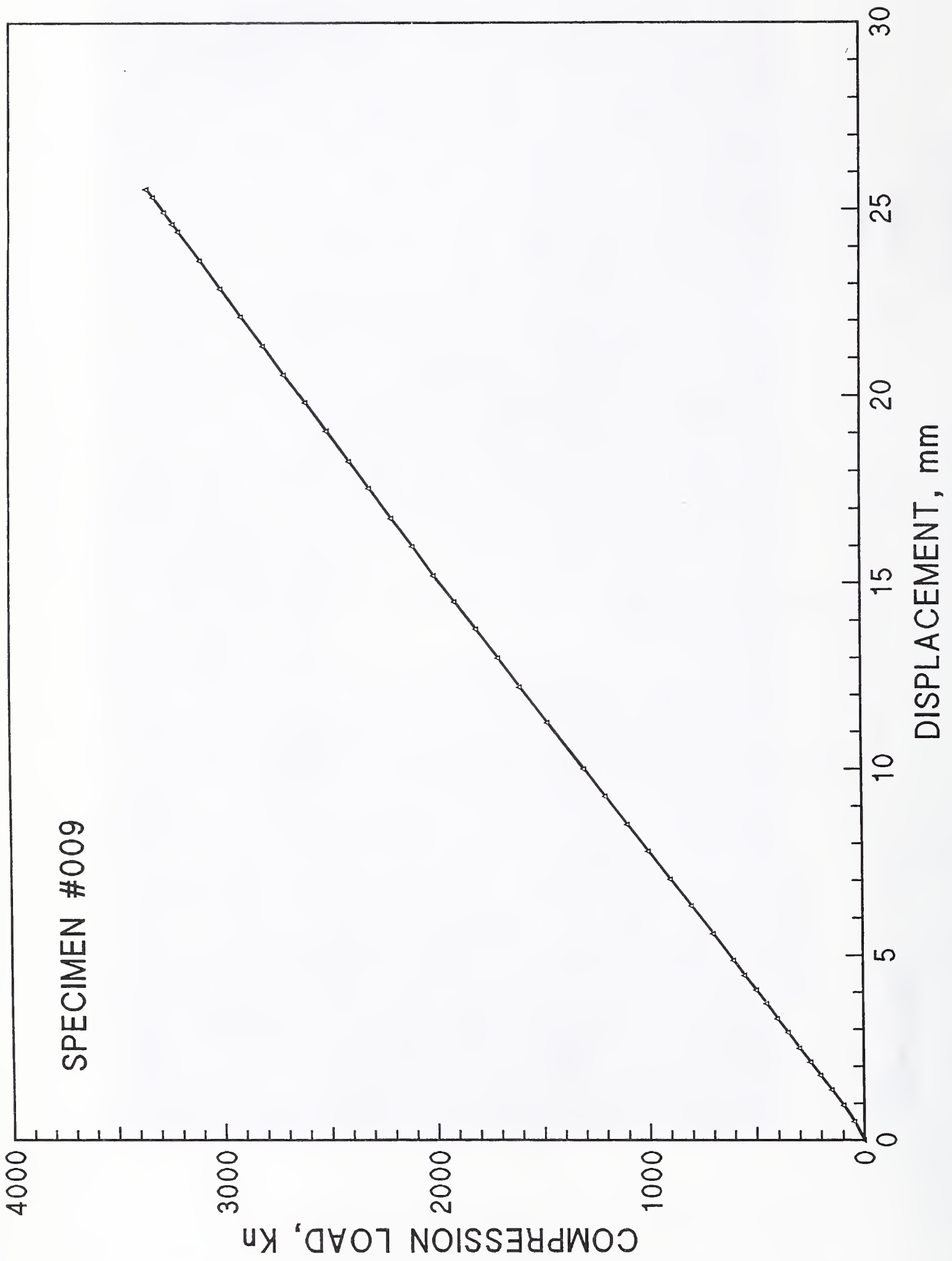
Figure 8. Load-versus-displacement curve for specimen 009.
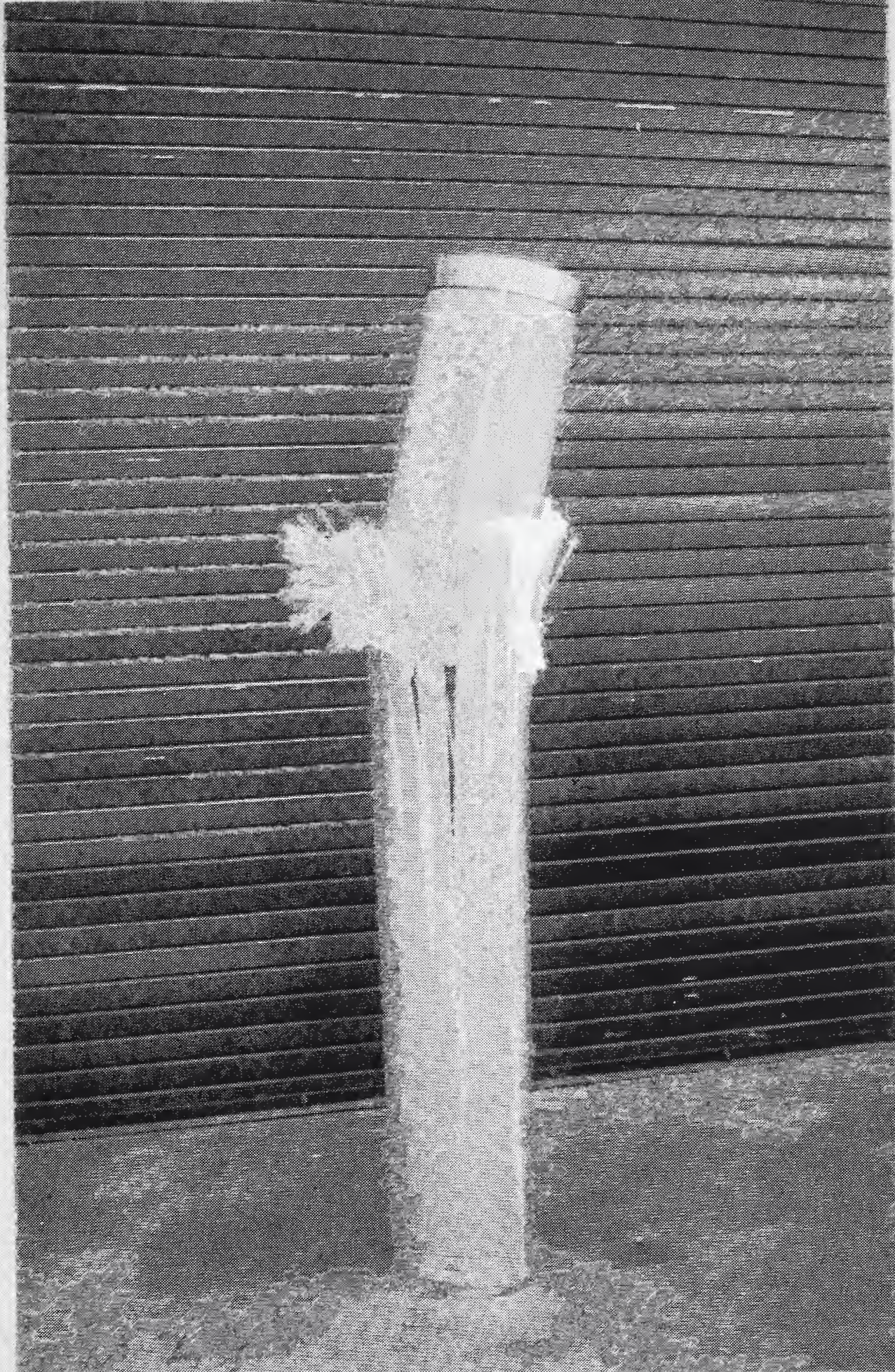
Figure 9.   Specimen 009 after ultimate strength test.

25
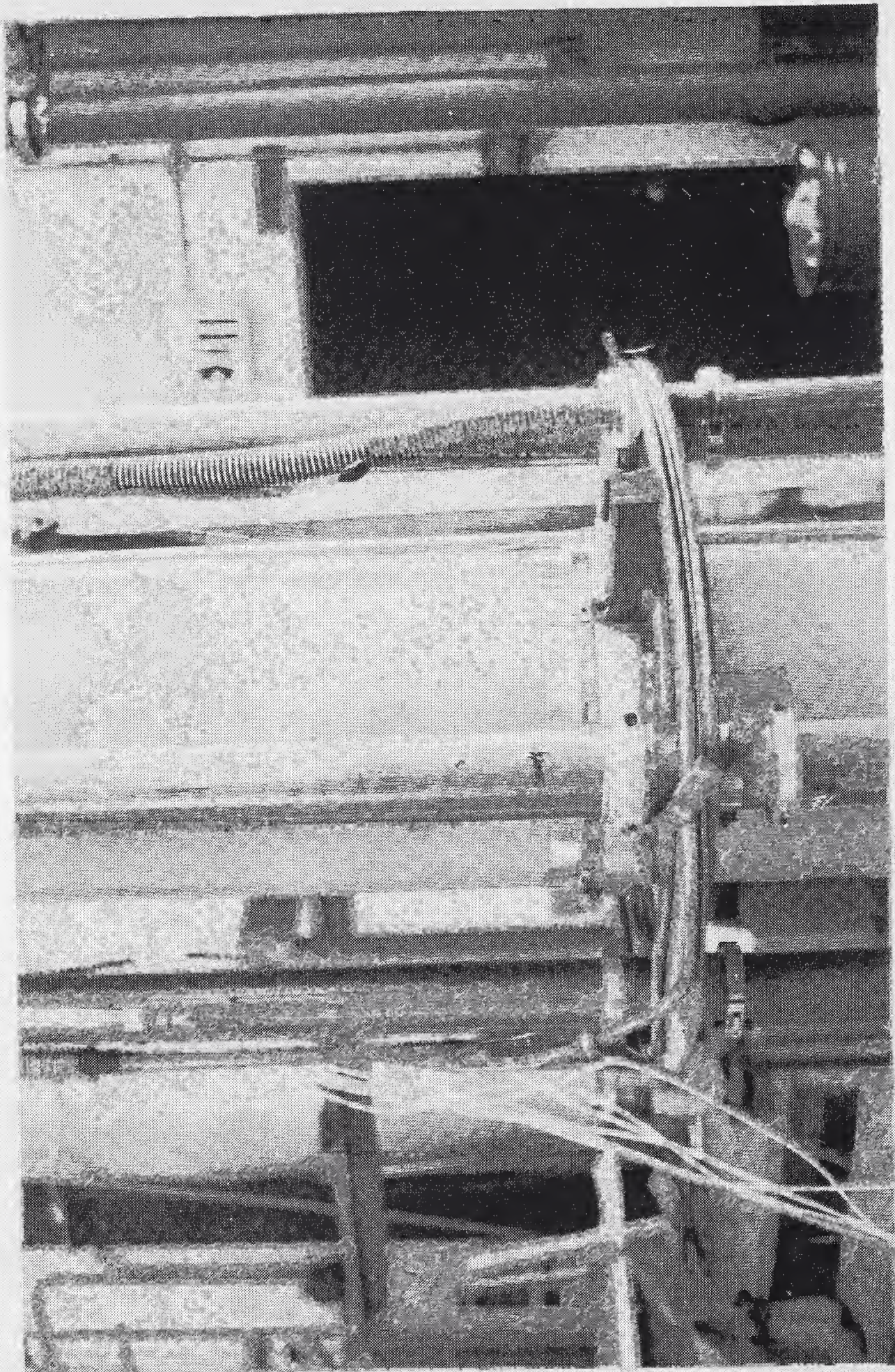
Figure 10.   Liquid nitrogen thermal intercept attachment.
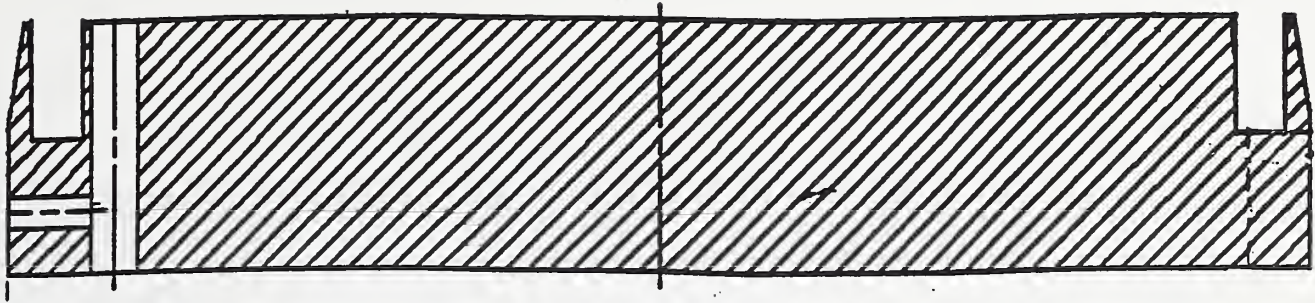
Figure 11A. Rigid aluminum end fitting (7075 Al).
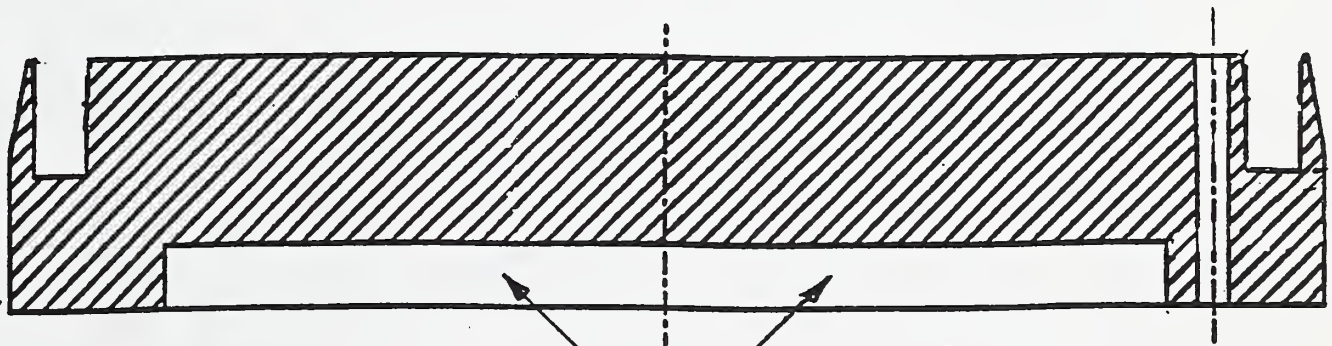
machined seat for lead plate

5 Aluminum
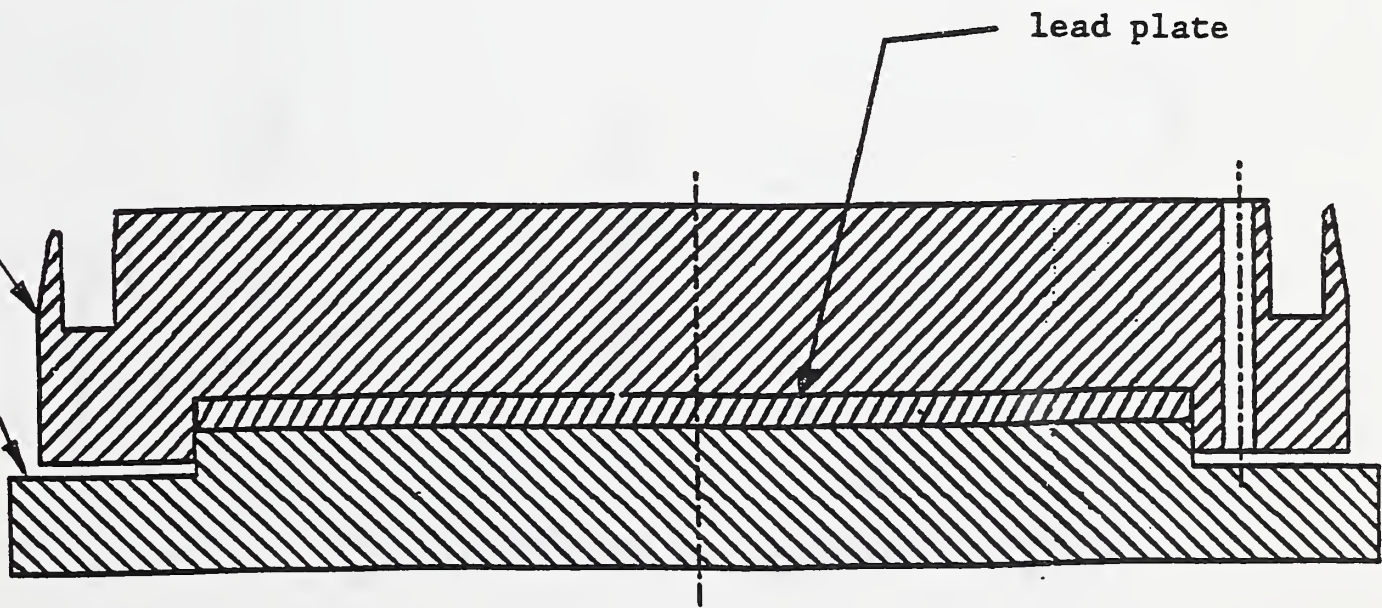
lead plate

Figure 11B. Self-aligning end fitting.
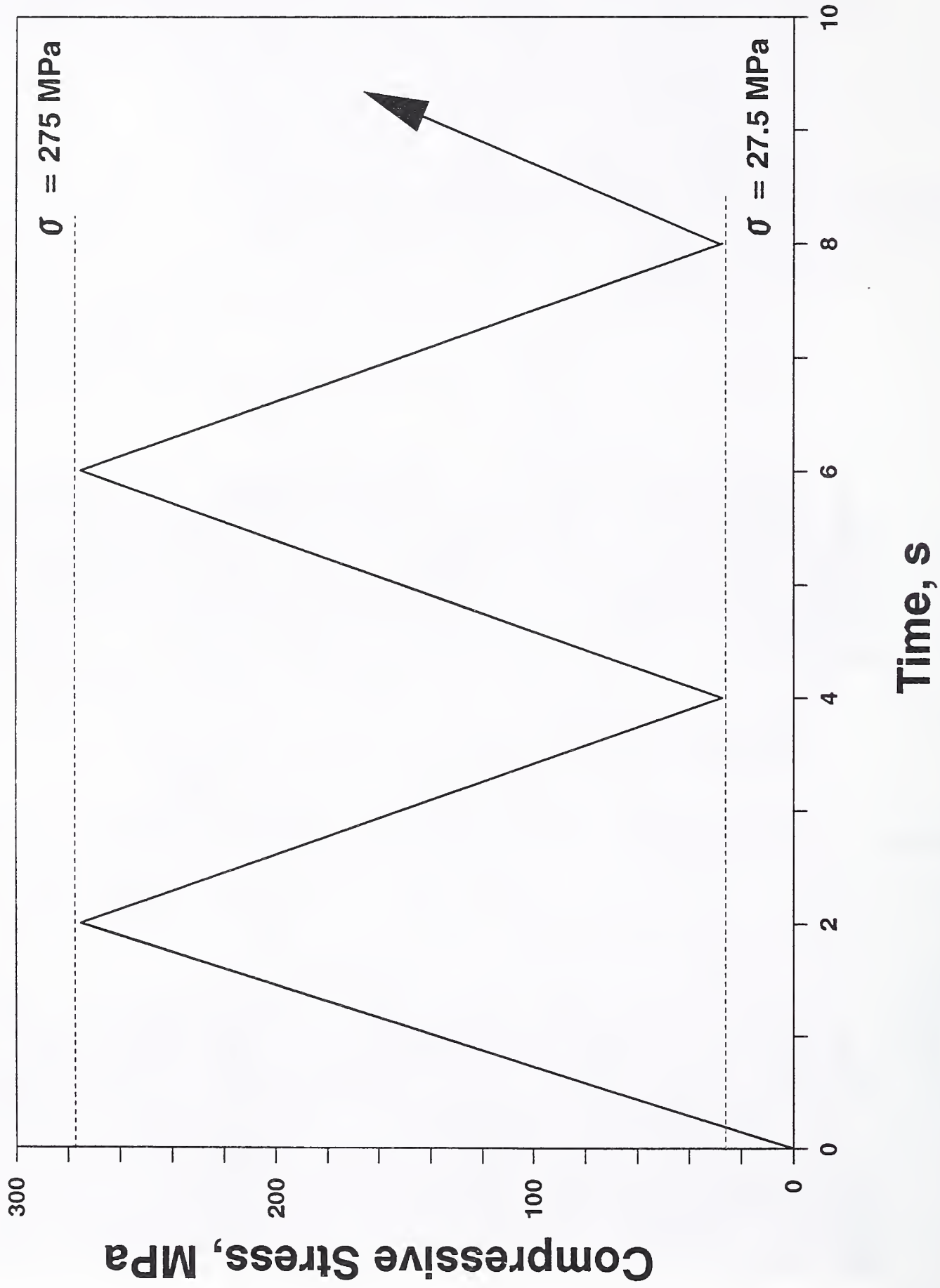
Figure 12. Schematic of fatigue test parameters for specimen 007.

28
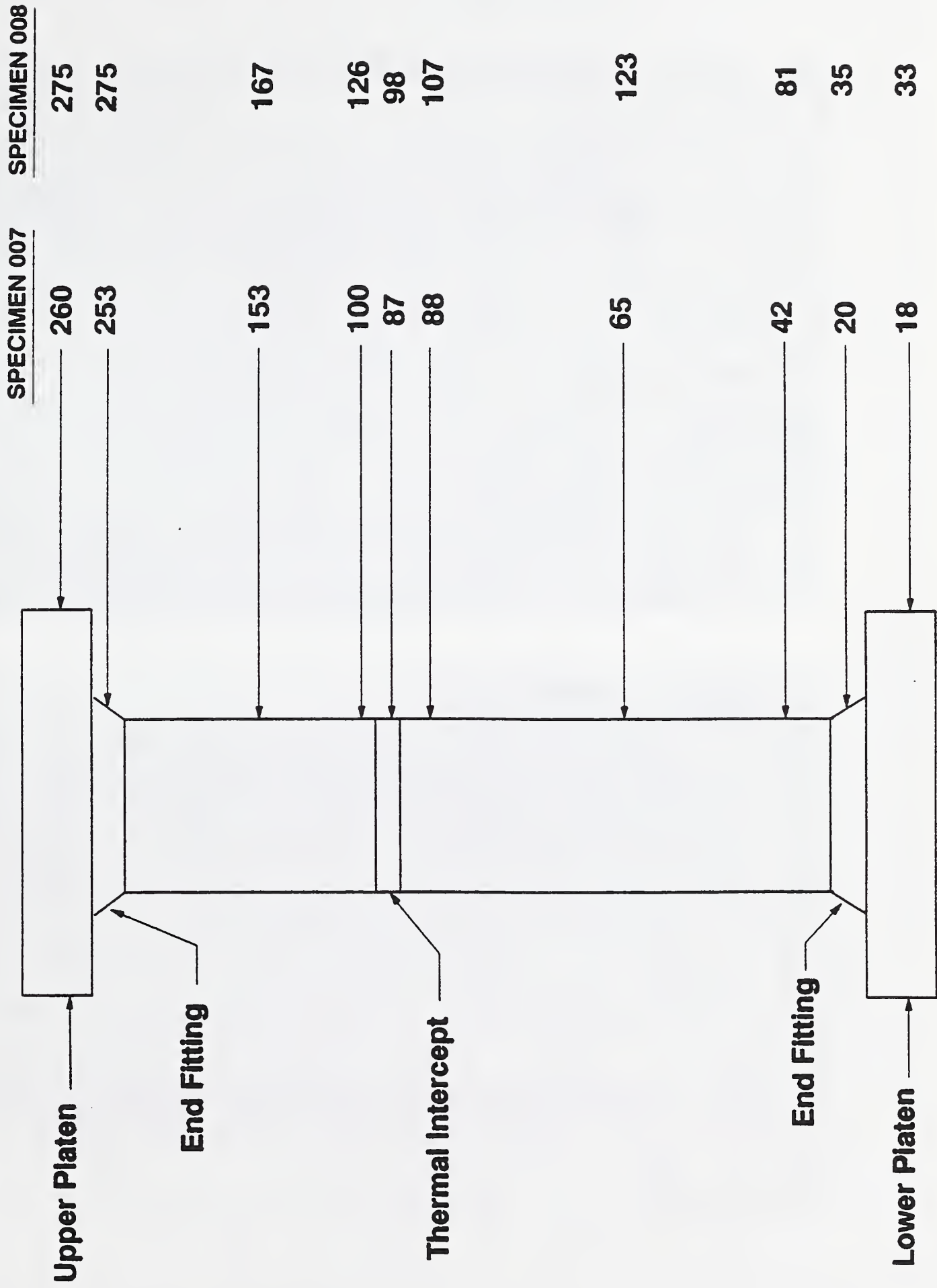
Figure 13.   Schematic for thermal gradient of specimens 007 and 008.
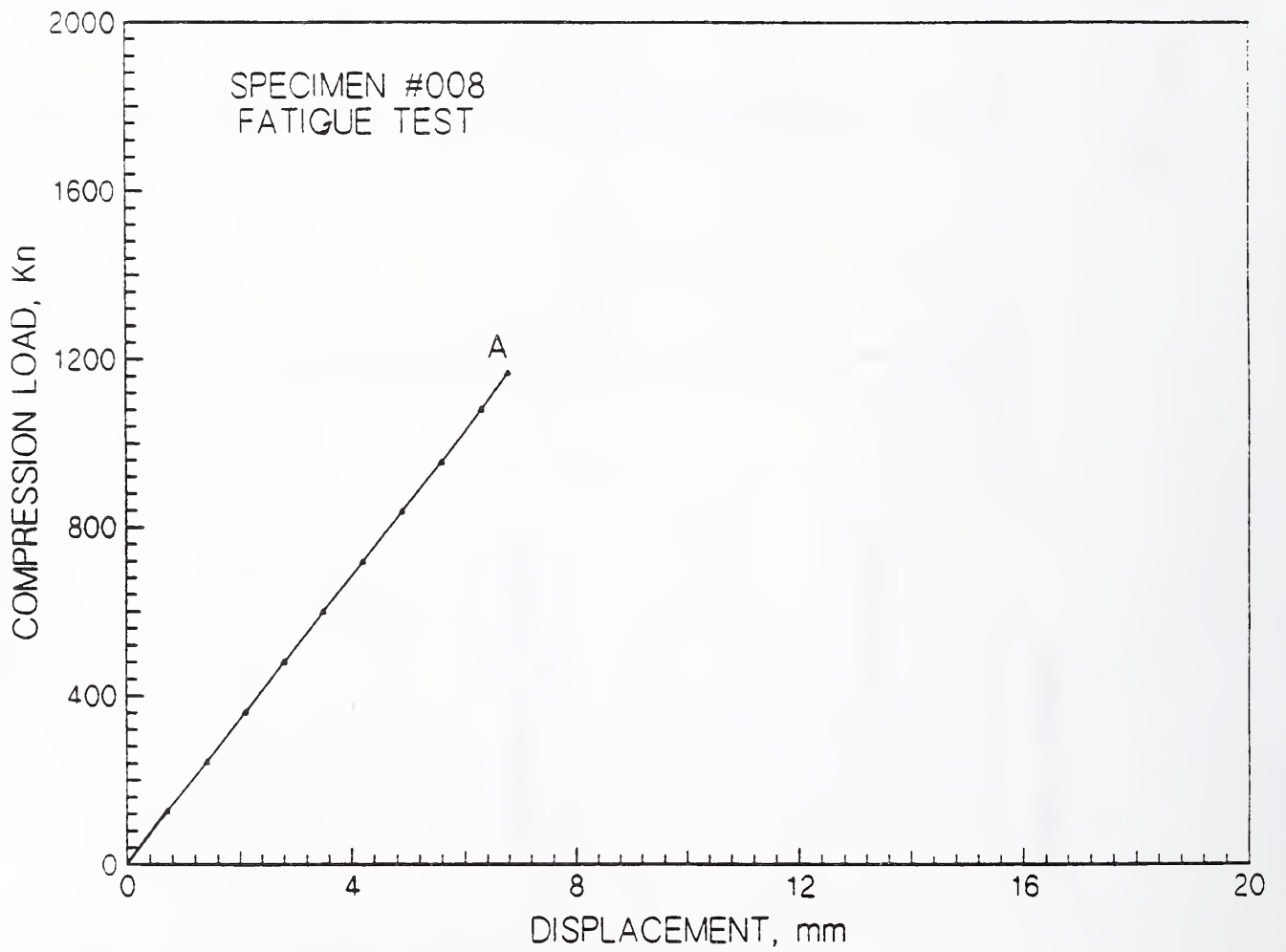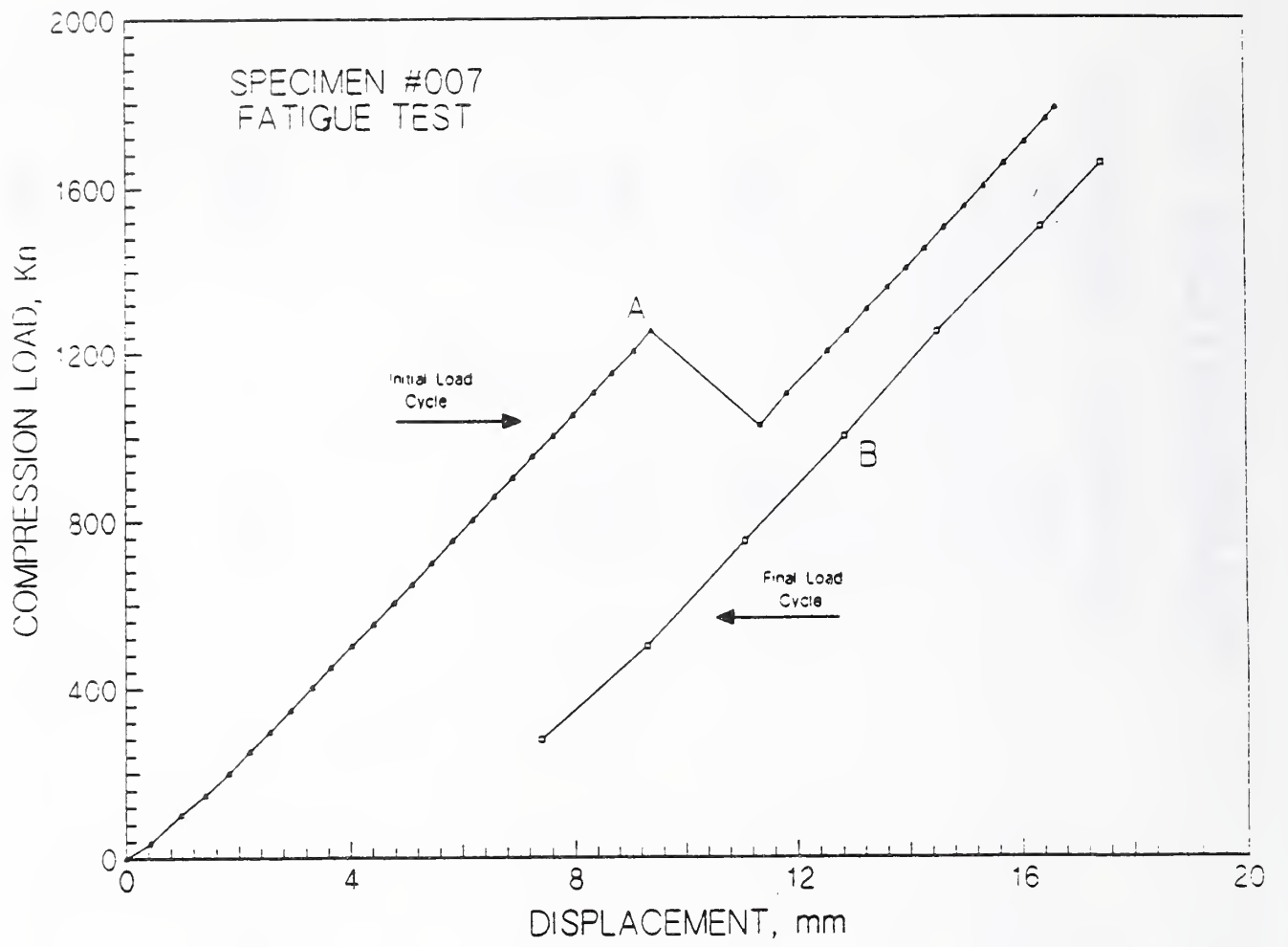
Figure 14. Load-versus-displacement curves for specimens 007 and 008.
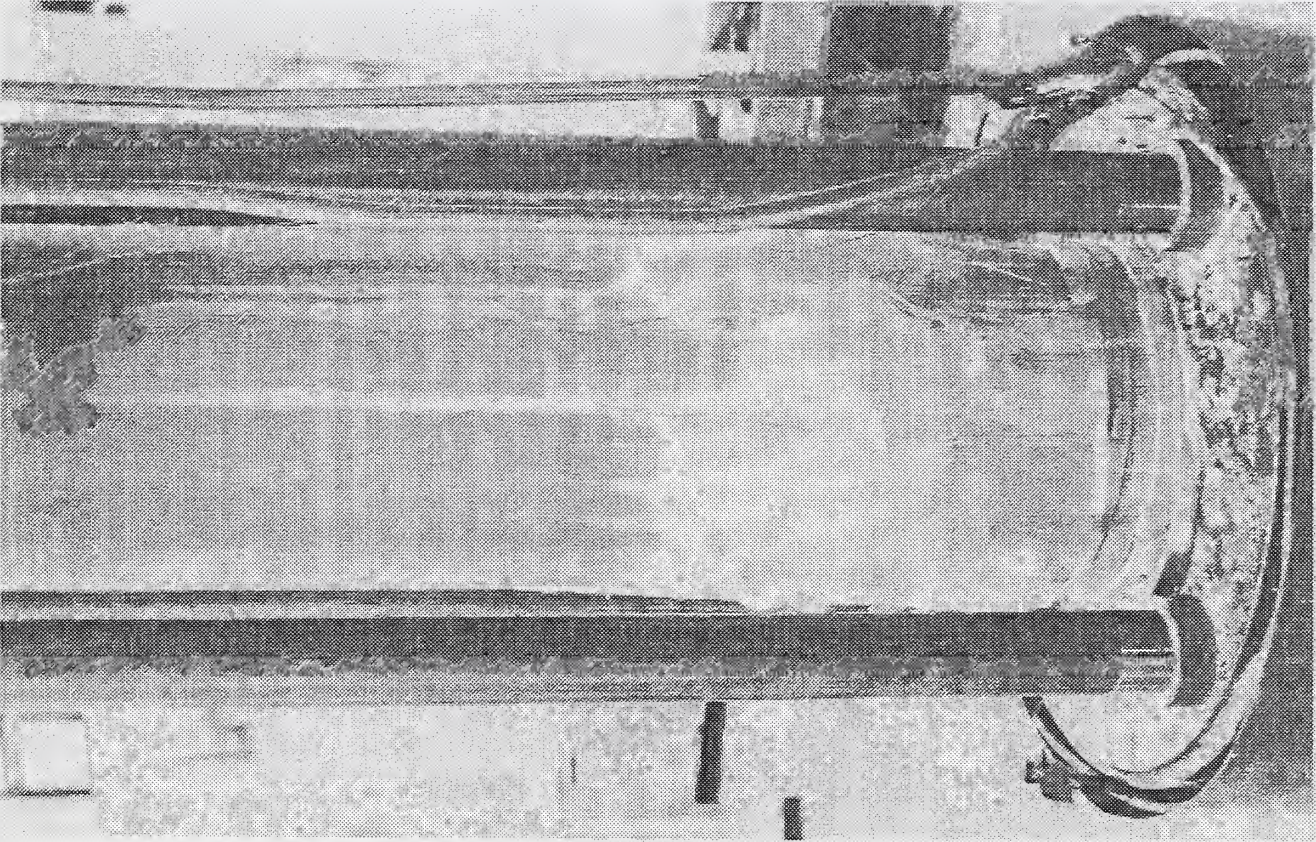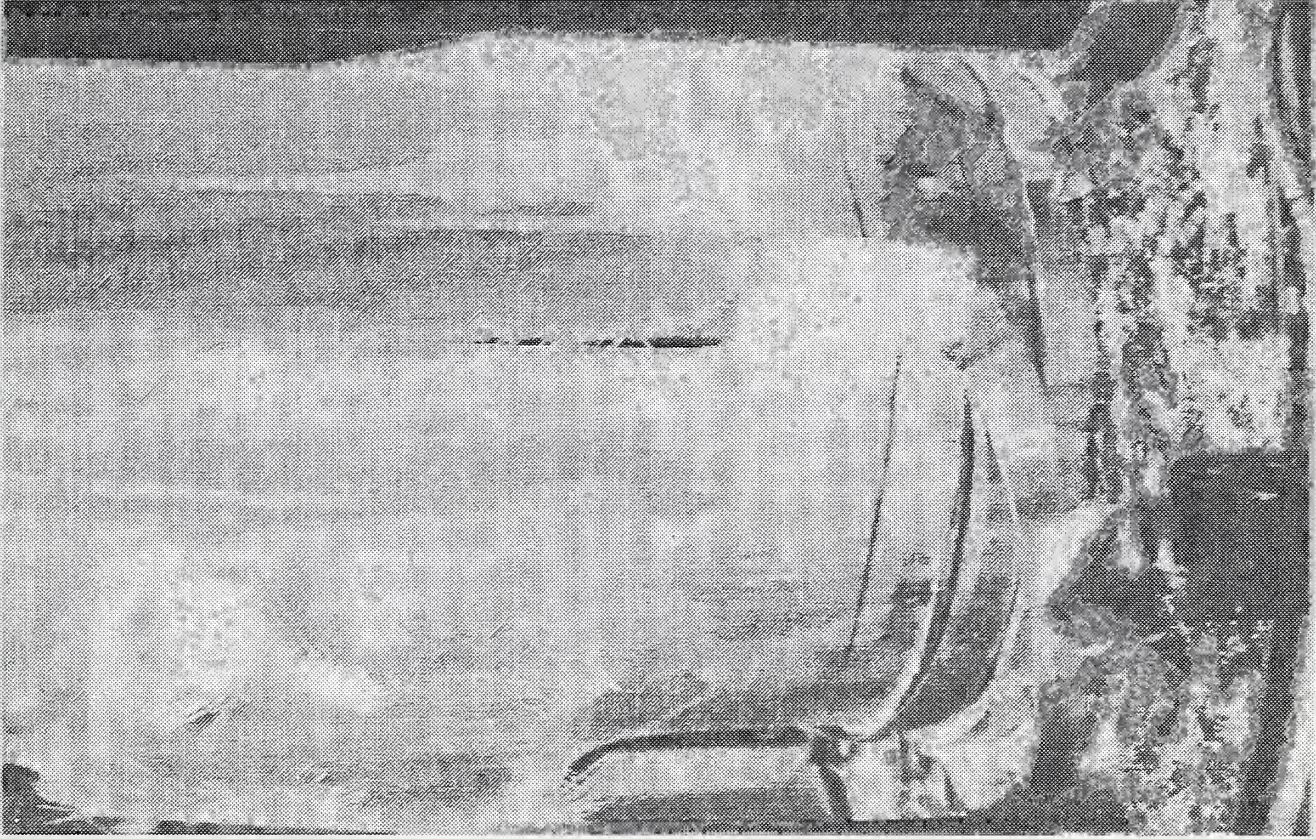
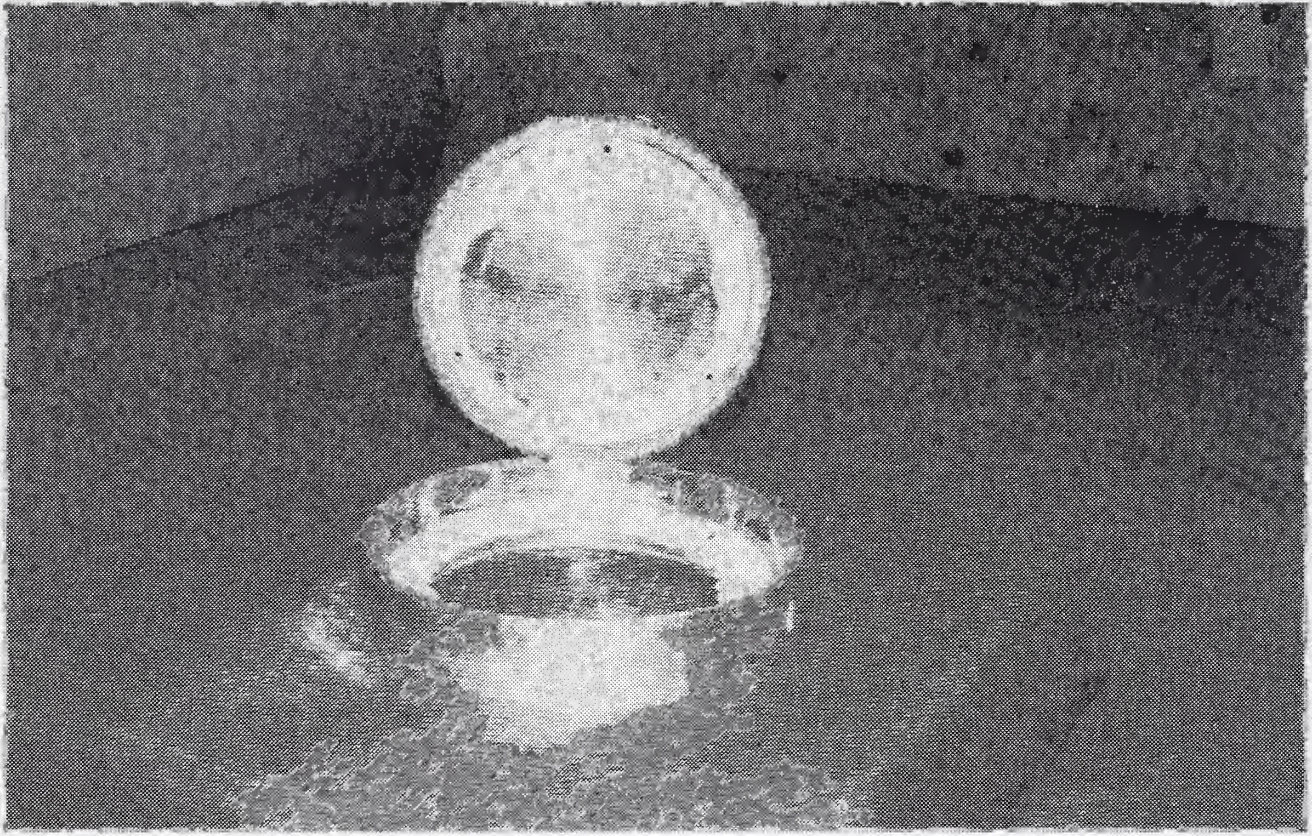Figure 15. Fatigue specimen 007, cold end failure.

Figure 16B.   A failed self-aligning end fitting, warm end of specimen 007.
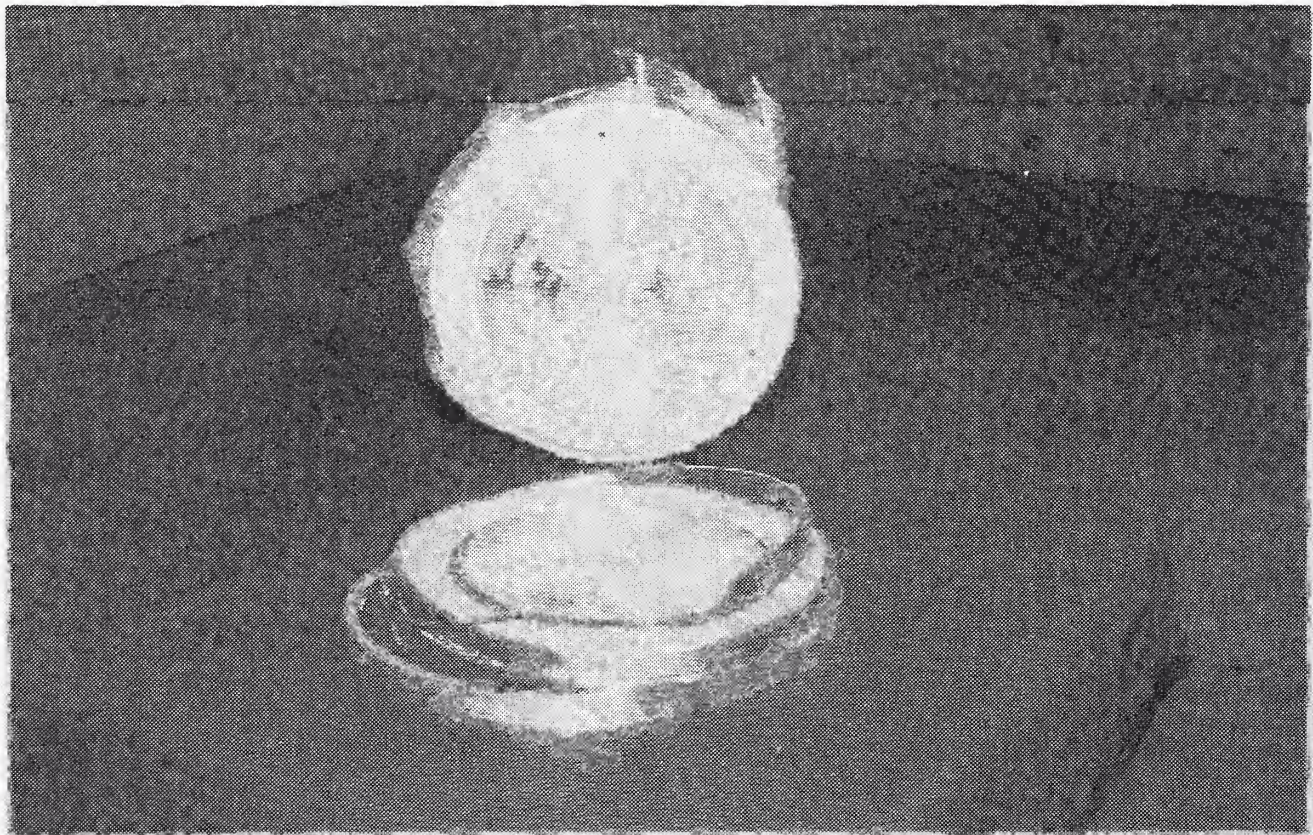

Figure 16A.   A failed self-aligning end fitting, cold end of specimen 007.

BL-114A (5-90) ADMAN 15.01	U.S. DEPARTMENT OF COMMERCE NATIONAL INSTITUTE OF STANDARDS AND TECHNOLOGY	1. PUBLICATION OR REPORT NUMBER NISTIR 3966
	BIBLIOGRAPHIC DATA SHEET	2. PERFORMING ORGANIZATION REPORT NUMBER B91-0161
		3. PUBLICATION DATE March 1992

4. TITLE AND SUBTITLE

A Cryogenic 4.4 MN Mechanical Test System for Large Scale Tests of Composite Support Struts

5. AUTHOR(S)

R.P. Walsh, R.P. Reed, J.D. McColskey, W. Fehringer, J.R. Berger

6. PERFORMING ORGANIZATION (IF JOINT OR OTHER THAN NIST, SEE INSTRUCTIONS) U.S. DEPARTMENT OF COMMERCE NATIONAL INSTITUTE OF STANDARDS AND TECHNOLOGY BOULDER, COLORADO 80303-3328	7. CONTRACT/GRANT NUMBER
	8. TYPE OF REPORT AND PERIOD COVERED

9. SPONSORING ORGANIZATION NAME AND COMPLETE ADDRESS (STREET, CITY, STATE, ZIP)

10. SUPPLEMENTARY NOTES

11. ABSTRACT (A 200-WORD OR LESS FACTUAL SUMMARY OF MOST SIGNIFICANT INFORMATION. IF DOCUMENT INCLUDES A SIGNIFICANT BIBLIOGRAPHY OR LITERATURE SURVEY, MENTION IT HERE.)

This report details a large mechanical test program undertaken by the NIST Materials Reliability Division. These tests were intended to validate the full scale structural behavior of the composite support struts in a thermal and mechanical environment identical to actual service conditions.

Two types of tests were performed: ultimate compressive strength and fatigue. Thermal conditions for the tests ranged from isothermal, room temperature tests to an imposed thermal gradient of cryogenic-to-room temperatures. The development of the unique facility necessary for the large scale cryogenic tests is detailed in this report.

12. KEY WORDS (6 TO 12 ENTRIES; ALPHABETICAL ORDER; CAPITALIZE ONLY PROPER NAMES; AND SEPARATE KEY WORDS BY SEMICOLONS)

composite; compressive platen; cryogenic; fiber-reinforced polymer; superconducting magnet; vacuum pump

13. AVAILABILITY	14. NUMBER OF PRINTED PAGES
X UNLIMITED	36
FOR OFFICIAL DISTRIBUTION. DO NOT RELEASE TO NATIONAL TECHNICAL INFORMATION SERVICE (NTIS).	
ORDER FROM SUPERINTENDENT OF DOCUMENTS, U.S. GOVERNMENT PRINTING OFFICE, WASHINGTON, DC 20402.	15. PRICE A03
X ORDER FROM NATIONAL TECHNICAL INFORMATION SERVICE (NTIS), SPRINGFIELD, VA 22161.	

ELECTRONIC FORM